PHARMA Pharmacologia

OPEN ACCESS

Unique Transcriptional Signatures Observed in Stem Cells from the Dental Pulp of Deciduous Teeth Produced on a Large Scale

[1,2]Rodrigo Pinheiro Araldi, [3]Mariana Viana, [2]Gabriel Avelar Colozza-Gama, [1,2,4]João Rafael Dias Pinto, [5]Lior Ankol, [3]Cristiane Wenceslau Valverde, [5]Eran Perlson and [1]Irina Kerkis

[1]BioDecision Analytics Limited, São Paulo, Brazil

[2]Paulista School of Medicine, Federal University of São Paulo, São Paulo, Brazil

[3]Cellavita Scientific Research Limited, Valinhos, São Paulo, Brazil

[4]Getulio Vargas Foundation, São Paulo, Brazil

[5]Sackler Faculty of Medicine, Tel-Aviv University, Tel Aviv-Yafo, Israel

ABSTRACT

Background and Objective: For sharing transcriptomic signatures with their origin, each population of mesenchymal stem/stromal cells (MSCs) exhibits unique properties. This study aimed to identify the transcriptomic signature of Human Immature Dental Pulp Stem Cells (hIDPSCs), a special type of MSC. **Materials and Methods:** To provide further evidence which may support the distinctive neuroprotective, neuroregenerative properties of hIDPSCs, it was performed the transcriptome analysis of these cells produced on a large-scale using RNA-Seq. Data were analyzed using bioinformatics tools to obtain the list of differentially expressed genes (DEGs). The DEGs identified in the hIDPSCs were subjected to functional enrichment analysis. **Results:** The data obtained were compared with the public data of RNA-Se from 136 samples from different donors of Adipocyte-Derived (AD-MSC), Bone Marrow (BM-MSC), Hepatocyte-Derived (HD-MSC), Menstrual Blood (MB-MSC), Umbilical Cord (UC-MSC) and Vertebral Tissue (vMSC) MSCs. These analyses showed that the hIDPSC shares at least 72% of transcripts with MSC from other sources. However, the cells have a unique transcriptional signature characterized by the differential expression of genes that promote axon growth and guidance. **Conclusion:** The unique transcriptional signature of the hIDPSCs provides evidence that the NestaCell® changes has neuro regenerative and neuroprotective actions, justifying the therapeutic effects we observed in both preclinical and clinical studies for neurodegenerative disorders.

KEYWORDS

NestaCell, RNA-Seq, neurogenesis, axon guidance, metabolic reprogramming

INTRODUCTION

The advent of cellular therapy has provided novel therapeutic opportunities for treating various incurable diseases, including neurodegenerative disorders[1-3]. This is because the therapeutic cells produce a multitude of bioactive molecules which can simultaneously target different pathways enrolled in the

ISSN: 2044-4656 (Online)
ISSN: 2044-4648 (Print)
https://doi.org/10.17311/pharmacologia.2023.72.95

Received: 14 Feb. 2023
Accepted: 15 Jun. 2023
Published: 01 Aug. 2023

pathophysiology of these diseases. In this scene, mesenchymal stromal/stem cells (MSCs) derived from bone marrow, adipocyte and other tissues are the most commonly studied class of Advanced Therapeutic Medicinal Product (ATMP), conferring multiple therapeutic benefits[1-3]. Moreover, the clinical safety of these cells has been provided in several metanalyses from 15 years of preclinical[4-7] and clinical studies for different diseases[8-11].

However, to share genetic and transcriptomic signatures with their origins, it is not surprising that MSCs derived from different tissues exhibit unique therapeutic properties which drive the clinical use of each type of MSC for a different set of diseases. In this context, the Human Immature Dental Pulp Stem Cells (hIDPSCs) emerge as a potential candidate for treating neurological disorders[1,3,12]. This is because, due to their ectomesenchymal origin (neural crest), the hIDPSCs produce high levels of Brain-Derived Neurotrophic Factor (BDNF) and nestin[13-15], proteins related to striatal neuron survival (BDNF)[16] and neuronal progenitor cell proliferation, differentiation and migration (nestin)[17], conferring neuroprotective and neuroregenerative properties to hIDPSCs[18-20]. However, despite their ectomesenchymal origin, the hIDPSCs have all the MSC phenotypical characteristics defined by the International Society for Cellular Therapy (ISCT)[21,22]. Furthermore, the hIDPSCs have anti-inflammatory properties three times higher than other typical MSCs[23,24]. Combined, these characteristics make these cells potential candidates for the treatment of neurodegenerative disorders, since the neurodegenerative process is closely related to neuroinflammation induced by mitochondrial dysfunctions[1,3].

Based on these advantages, Kerkis *et al.*[18] developed an innovative method to isolate hIDPSCs from the dental pulp of deciduous teeth from children aged between 6-12 years. This technology, which allows scaling up the hIDPSCs production for therapeutic use[25], was patented (patent US9790468B2) and licensed by the Cellavita Scientific Research Ltd., a Brazilian company that has produced these cells under good manufacturing process (GMPs) for clinical use. The hIDPSCs, in thefifth passage, produced by the Cellavita correspond to the active component of the NestaCell® product.

In previous preclinical studies, we showed that the active component of the NestaCell® product (hIDPSCs) can cross the brain-blood barrier and homing within the subventricular zone and striatum of rats subjected to the systemic treatment with 3-nitroproprionic acid (3-NP) – an animal model for Huntington's disease (HD)[1,14,20]. In addition, the NestaCell® product can restore the expression of BNDF (which is involved in both HD and amyotrophic lateral sclerosis (ALS) pathophysiology), DARPP32 and D2R (markers of medium spiny neurons) in the striatum of rats treated with 3-NP when compared with placebo (saline) was also noted[25,26]. These results provide evidence that the hIDPSCs have neuroprotective and neuroregenerative properties[1,14,20]. Reinforcing these findings, in another independent preclinical study with rats intrastriatal treated with 6-hydrodopamine (6-OHDA)-an animal model for Parkinson's disease (PD), the intravenous treatment with the NestaCell® product was improved motor, cognitive and neuropsychiatric functions only three days after the hIDPSC transplantation was also observed[27]. These results were also confirmed in both Phase I and II clinical trials for HD (NCT02728115 and NCT03252535).

Considering these results, this study aimed to compare the transcriptome of the hIDPSCs with other 136 samples from different donors of adipocyte-derived (AD-MSC), bone marrow (BM-MSC), hepatocyte-derived (HD-MSC), menstrual blood (MB-MSC), umbilical cord (UC-MSC) and vertebral tissue (vMSC) MSCs-all provided from SRA Database to identify the differentially expressed genes (transcriptional signature) that can justify the preclinical and clinical results as described.

MATERIALS AND METHODS

Ethical approval: The deciduous teeth (dental pulp) and cell isolation as well as their use present study were approved by Brazilian's National Ethics Committee (process number 066/2018), following all applicable regulations. Informed consent was obtained from each donor and signed by the parents of the

children. The children received comprehensive expiation about the use of their cells for biological research. The hIDPSCs isolation and expansion were performed at Cellavita Scientific Research Ltda. (Valinhos, São Paulo, Brazil) RNA-Seq and bioinformatic analysis were performed at the Genetics Laboratory of Butantan Institute (São Paulo, Brazil) All analysis were performed between May and December, 2022.

Cell culture: Human Immature Dental Pulp Stem Cells (hIDPSCs) were obtained from the dental pulp of deciduous teeth collected from four children aged between 6-12 years, with no previous diagnosis of genetic diseases, following informed consent, as described by Kerkis *et al.*[18]. Briefly, hIDPSCs were seeded into culture flasks (150-cm^2, Corning, New York, USA) in Dulbecco's modified Eagle's medium (DMEM)/Ham's F12 (1:1; Invitrogen, Carlsbad, California, USA), supplemented with 15% fetal bovine serum (FBS; HyClone, Logan, Utah, USA), 2 mM glutamine (Gibco, Gaithersburg, Maryland, USA), 50 mg mL^{-1} gentamicin sulfate (Schering-Plough, Whitehouse Station, New Jersey, USA) and 1% nonessential amino acid (Gibco, Carlsbad, California, USA). Cultures were incubated at 37°C in a 5% CO_2 humidity atmosphere. Cells were expanded until the fifth passage (which corresponds to the active component of the NestaCell® product). The medium was changed every two days and the cells were grown until they reached semi-confluence (80-90%). In the fifth passage, the cells were harvested and cryopreserved according to the manufacturing process of the NestaCell® product, which was patented (patent US9790468B2).

The hIDPSCs used in this study express the typical MSC markers proposed by the International Society for Cellular and Gene Therapy (ISCGT)[21], being positive for CD105, CD73, CD90 and CD44 and negative for CD45, CD34, CD14 and HLA class II[13,15,18,25,28]. Additionally, we also showed that these cells highly express a set of neurotrophic factors, including BDNF, nestin, Nerve Growth Factor (NGF) and neurotrophins 3 and 4 (NT-3 and NT-4)[14,20,29,30].

For this study, four batches of the NestaCell® product (identified as NestaCell_batch1 to NestaCell_batch4) were used. Each batch was obtained from a different donor.

RNA extraction, library construction and sequencing: Total RNA from hIDPSCs (NestaCell® product) was extracted using TRIzol reagent (Invitrogen, Carlsbad, California, USA), according to the manufacture's protocol. The RNA was digested with DNase I (New England Biolabs, Ipwich, Massachusetts, USA) to remove genomic DNA. The RNA concentration was quantified spectrophotometrically using the Nanodrop ND-1000 (Thermo Fisher Scientific, Carlsbad, California, USA) and its quality and integrity were assessed by capillary electrophoresis on an Agilent 2100 BioAnalyzer system (Agilent, Santa Clara, California, USA) with an RNA integrity number (RIN) >7, as recommended by Conesa *et al.*[30]. The cDNA libraries were prepared with 1 µg of starting total RNA using the TrueSeq RNA Library Prep Kit (Illumina Inc., San Diego, California, USA). The libraries were amplified via 15 cycles of PCR and the amplified library was sequenced using an Illumina HiSeq 2000. The paired-end sequencing was performed with a read depth of 50 million reads per sample/batch. Both library preparation and sequencing were performed by CD Genomics (Shirley, New York, USA).

Sequencing annotation and identification of differentially expressed genes (DEGs): The FASTQ-formatted sequencing data (deposited in the SRA database, BioProject ID PRJNA925198, Submission ID SUB12342309) were de-multiplexed to assign reads to the originated samples. Raw sequence quality control was performed using FastQC version 0.11.9 reads and was mapped to the human genome reference Grch38.p13 version GTF v.103 using STAR[31]. The total mapped read number for each transcript was normalized using DESeq2 version 1.36.0, as described by Love *et al.*[32]. Genes with low counts were filtered out using the proportion test (method 3) of the NOISeq package version 2.40.0, as proposed by Tarazona *et al.*[33]. To compare the transcriptome of the active component of the NestaCell® product with the transcriptome of other 136 samples from MSCs derived from different tissue sources

(Table 1), we performed a multidimensional scaling (MDS) plot, based on an unsupervised dimensionality reduction technique of the Uniform Manifold Approximation and Projection (UMAP)[34] as an approach to visualize the data structure of the analyzed samples, as proposed by Lamas *et al.*[35]. The DEG analysis was conducted with only transcripts with log2-fold change. This allowed us to focus only on genes at least two-fold expressed by the active component of NestaCell® product (hIDPSCs) compared to all other MSC (log2FC>1). All analysis was performed by using R version 4.2.2.

Table 1: Results of quality control, reads alignment and feature counts

	Project/sample identification		Quality control		Aligned reads (M)[1]		
CMT	BioProject	Sample	Phred score	Accuracy	1	2	Total feature counts (M)[2]
NestaCell® (hIDPSCs)	PRJNA925198	SAMN32783909	36	>99.99%	67.69	17.60	19.30
		SAMN32783910	36	>99.99%	55.26	21.00	18.00
		SAMN32783911	36	>99.99%	24.29	23.10	34.30
		SAMN32783912	36	>99.99%	26.35	24.90	34.90
AD-MSC		Donor 1[3]	36	>99.99%	26.01	25.20	43.30
		Donor 2[3]	36	>99.99%	20.64	19.40	33.10
AD-MSC	PRJNA576920	SRR10262855	36	>99.99%	14.52	13.10	23.20
		SRR10262856	36	>99.99%	14.52	13.10	23.20
		SRR10262857	36	>99.99%	14.08	12.70	22.50
		SRR10262858	36	>99.99%	14.30	12.90	22.90
		SRR10262863	36	>99.99%	8.34	7.20	11.70
		SRR10262864	36	>99.99%	12.30	10.60	17.30
		SRR10262865	36	>99.99%	11.69	10.10	16.40
		SRR10262866	36	>99.99%	11.57	10.00	16.30
		SRR10262867	36	>99.99%	11.96	10.30	16.80
		SRR10262868	36	>99.99%	10.76	9.30	15.10
		SRR10262869	36	>99.99%	11.00	9.50	15.50
		SRR10262870	36	>99.99%	11.36	9.80	16.00
		SRR10262871	36	>99.99%	8.35	7.20	11.60
		SRR10262872	36	>99.99%	8.23	7.10	11.60
		SRR10262873	36	>99.99%	8.11	7.00	11.30
		SRR10262874	36	>99.99%	8.11	7.00	11.40
		SRR10262875	36	>99.99%	8.23	7.10	11.50
		SRR10262876	36	>99.99%	8.35	7.20	11.70
		SRR10262877	36	>99.99%	7.89	6.80	11.10
		SRR10262878	36	>99.99%	11.94	10.30	16.70
	PRJEB36449	ERR3841974	36	>99.99%	29.33	27.60	49.40
		ERR3841975	36	>99.99%	20.19	18.90	33.50
		ERR3841976	36	>99.99%	25.42	24.00	42.30
		ERR3841977	36	>99.99%	26.58	25.30	44.80
		ERR3841978	36	>99.99%	29.65	27.90	49.70
		ERR3841979	36	>99.99%	28.63	27.00	47.20
		ERR3841980	36	>99.99%	31.42	29.50	49.10
		ERR3841981	36	>99.99%	26.38	25.30	44.60
BM-MSC		Donor 1[3]	36	>99.99%	24.69	23.90	30.60
BM-MSC	PRJNA576920	SRR10262769	36	>99.99%	13.68	12.50	22.20
		SRR10262770	36	>99.99%	13.68	12.50	22.40
		SRR10262771	36	>99.99%	13.35	12.20	21.70
		SRR10262772	36	>99.99%	13.46	12.30	21.90
		SRR10262777	36	>99.99%	12.13	10.60	17.50
		SRR10262778	36	>99.99%	21.49	18.80	31.10
		SRR10262779	36	>99.99%	20.55	18.00	29.70
		SRR10262780	36	>99.99%	20.32	17.80	29.40
		SRR10262781	36	>99.99%	20.96	18.30	30.10
		SRR10262782	36	>99.99%	19.16	16.80	27.70
		SRR10262783	36	>99.99%	19.61	17.20	28.30
		SRR10262784	36	>99.99%	20.11	17.60	29.00

Table 1: Continue

CMT	Project/sample identification		Quality control		Aligned reads (M)[1]		Total feature counts (M)[2]
	BioProject	Sample	Phred score	Accuracy	1	2	
		SRR10262785	36	>99.99%	12.11	10.60	17.40
		SRR10262786	36	>99.99%	12.00	10.50	17.30
		SRR10262849	36	>99.99%	11.77	10.30	16.90
		SRR10262850	36	>99.99%	11.77	10.30	16.90
		SRR10262851	36	>99.99%	11.89	10.40	17.10
		SRR10262852	36	>99.99%	12.13	10.60	17.40
		SRR10262853	36	>99.99%	11.54	10.10	16.50
		SRR10262854	36	>99.99%	21.03	18.40	30.30
	PRJNA740003	SRR14903835	36	>99.99%	35.39	34.40	62.10
		SRR14903839	36	>99.99%	32.78	31.80	57.40
	PRJEB50630	ERR8382149	36	>99.99%	16.99	14.90	27.40
		ERR8382150	36	>99.99%	16.46	14.50	26.80
		ERR8382151	36	>99.99%	15.82	14.00	25.70
		ERR8382152	36	>99.99%	16.87	14.90	27.50
		ERR8382153	36	>99.99%	15.20	12.10	22.30
		ERR8382154	36	>99.99%	17.57	15.30	28.20
		ERR8382155	36	>99.99%	17.66	15.70	28.90
		ERR8382156	36	>99.99%	18.31	16.30	29.90
	PRJEB44754	ERR5881993	36	>99.99%	30.68	27.80	50.40
		ERR5881994	36	>99.99%	33.74	30.70	55.50
		ERR5881995	36	>99.99%	33.11	29.30	54.10
		ERR5881996	36	>99.99%	41.23	37.40	67.80
		ERR5881997	36	>99.99%	34.91	32.40	60.00
UC-MSC	PRJNA721023	SRR14203521	36	>99.99%	30.68	27.80	50.40
		SRR14203515	36	>99.99%	33.74	30.70	55.50
		SRR14203509	36	>99.99%	33.11	29.30	54.10
		SRR14203503	36	>99.99%	41.23	37.40	67.80
		SRR14203496	36	>99.99%	34.91	32.40	60.00
		SRR14203489	36	>99.99%	34.30	31.80	57.20
		SRR14203483	36	>99.99%	29.57	28.30	51.00
		SRR14203476	36	>99.99%	44.38	42.60	76.90
		SRR14203517	36	>99.99%	24.14	23.10	41.30
		SRR14203511	36	>99.99%	60.94	58.50	104.50
		SRR14203505	36	>99.99%	26.67	25.50	46.10
		SRR14203498	36	>99.99%	36.46	34.60	62.20
		SRR14203492	36	>99.99%	25.10	24.00	43.30
		SRR14203485	36	>99.99%	28.17	27.10	49.10
		SRR14203514	36	>99.99%	29.05	26.70	48.40
		SRR14203507	36	>99.99%	27.04	24.20	42.40
		SRR14203500	36	>99.99%	32.04	30.60	55.30
		SRR14203494	36	>99.99%	24.00	22.80	41.00
		SRR14203487	36	>99.99%	32.22	29.90	53.50
		SRR14203481	36	>99.99%	44.76	43.10	77.70
		SRR14203524	36	>99.99%	47.68	45.30	80.70
		SRR14203523	36	>99.99%	48.40	45.30	79.80
	PRJNA576920	SRR10262903	36	>99.99%	12.42	11.40	20.50
		SRR10262904	36	>99.99%	12.75	11.70	21.00
		SRR10262905	36	>99.99%	12.96	11.90	21.50
		SRR10262906	36	>99.99%	12.75	11.70	21.20
		SRR10262972	36	>99.99%	16.07	14.70	25.20
		SRR10262973	36	>99.99%	16.83	15.40	26.40
		SRR10262974	36	>99.99%	16.81	15.40	26.50
		SRR10262975	36	>99.99%	18.25	16.70	28.70
		SRR10262976	36	>99.99%	16.50	15.10	25.90
		SRR10262977	36	>99.99%	16.72	15.30	26.30
		SRR10262978	36	>99.99%	16.94	15.50	26.60
		SRR10262979	36	>99.99%	17.05	15.60	26.80

Table 1: Continue

	Project/sample identification		Quality control		Aligned reads (M)[1]		
CMT	BioProject	Sample	Phred score	Accuracy	1	2	Total feature counts (M)[2]
MB-MSC	PRJNA742515	SRR14999064	36	>99.99%	18.84	17.80	24.70
		SRR14999065	36	>99.99%	20.90	19.60	27.30
		SRR14999066	36	>99.99%	21.28	20.00	26.90
		SRR14999067	36	>99.99%	28.00	25.90	18.40
HD-MSC	PRJNA576920	SRR10262879	36	>99.99%	18.62	16.70	30.00
		SRR10262880	36	>99.99%	18.62	16.70	30.10
		SRR10262881	36	>99.99%	18.06	16.20	29.10
		SRR10262882	36	>99.99%	18.39	16.50	29.60
		SRR10262887	36	>99.99%	11.50	9.30	15.30
		SRR10262888	36	>99.99%	16.60	13.40	22.30
		SRR10262889	36	>99.99%	15.80	12.80	21.30
		SRR10262890	36	>99.99%	15.68	12.70	21.10
		SRR10262891	36	>99.99%	16.13	13.00	21.50
		SRR10262892	36	>99.99%	14.57	11.80	19.70
		SRR10262893	36	>99.99%	14.92	12.10	20.20
		SRR10262894	36	>99.99%	15.45	12.50	20.70
		SRR10262895	36	>99.99%	11.51	9.30	15.40
		SRR10262896	36	>99.99%	11.39	9.20	15.30
		SRR10262897	36	>99.99%	11.14	9.00	14.90
		SRR10262898	36	>99.99%	11.11	9.00	14.80
		SRR10262899	36	>99.99%	11.26	9.10	15.10
		SRR10262900	36	>99.99%	11.52	9.30	15.30
		SRR10262901	36	>99.99%	10.89	8.80	14.70
		SRR10262902	36	>99.99%	16.07	13.00	21.60
vMSC	PRJNA576920	SRR10262996	36	>99.99%	10.32	9.60	17.20
		SRR10262997	36	>99.99%	10.54	9.80	17.50
		SRR10262998	36	>99.99%	10.87	10.10	18.00
		SRR10262999	36	>99.99%	10.66	9.90	17.70
		SRR10263004	36	>99.99%	10.39	9.40	15.70
		SRR10263005	36	>99.99%	10.50	9.50	16.00
		SRR10263006	36	>99.99%	10.49	9.50	15.90
		SRR10263007	36	>99.99%	10.83	9.80	16.40
		SRR10263008	36	>99.99%	10.39	9.40	15.80
		SRR10263009	36	>99.99%	10.50	9.50	15.90
		SRR10263010	36	>99.99%	10.50	9.50	15.90
		SRR10263011	36	>99.99%	10.39	9.40	15.80

[1]Number of reads (in million-M) aligned per sequencing, [2]Total of reads mapped in paired-end sequencing, Samples donated by Prof. Dr, Sérgio Bydlkowky (FM-USP, São Paulo, Brazil) and sequenced by us (data available from SRA database), hIDPSC: Human immature dental pulp stem cells; AD-MSC: Adipocyte-derived mesenchymal stem cells, BM-MSC: Bone marrow mesenchymal stem cells, MB-MSC: Menstrual blood mesenchymal stem cells, UC-MSC: Unbilical cord mesenchymal stem cells, HD-MSC: Hepatocyte-derived mesenchymal stem cells and vMSC: Vertebral mesenchyma stem cells

Gene ontology (GO) and functional enrichment analysis: To understand the biological impact of the DEGs, we performed functional enrichment analysis through over-representation (ORA) method, using the KEGG and PANTHER database available on the functional enrichment analysis tool version 3.1.4 (FunRich)and Web-based Gene SeT Analysis Toolkit (WebGestalt,) with a false discovery ratio (FDR) of 0.95 and adjusted p-valor of 0.05.

Axon guidance analysis: To confirm the RNA-Seq results, we treated primary spinal cord neurons (motor neurons-MN) from E12.5 mouse embryos of inducible doxycycline (Dox)-suppressible expression of human transactivation-responsive DNA-binding protein of 43 kDa (NEFH-hTDP-43ΔNLS mice, stock number 028412)[36] with different concentrations (25, 50 and 100 μg mL^{-1}) of exosomes isolated from conditioned culture medium of the hIDPSCs (NestaCell® product). For this assay, we used the exosomes because (I) Culture medium of primary spinal cord neurons is different from the culture medium of

hIDPSCs, which could change the hIDPSCs expression, while the exosome cargo is not affected by the environmental conditions and (II) Exosomes acts as a natural vehicle to deliver active biomolecules to recipient cells. In detail: The MNs were seeded and maintained in a 96-well plate containing 200 µL of complete Neurobasal (CNB) medium containing Neurobasal, 4% B27, 2% horse serum (Biological Industries), 1% Glutamax, 1% P/S, 25 µM Beta-Mercapto ethanol, 25 ng mL^{-1} BDNF, 1 ng mL^{-1} GDNF (Alomone) and 0.5 ng mL^{-1} CNTF (Alomone).

The MNs were seeded at a density of 10,000 cells per well. The media with the suitable treatment was replaced every two days. The exosomes were isolated from the conditioned culture medium of the hIDPSCs by ultracentrifugation using the ultracentrifugation-based method developed by Narbute *et al*.[37]. The exosomal nature of the extracellular vesicles isolated using our method was confirmed by nanoparticle tracking analysis (which show that the vesicles have a medium diameter of 120 nm) and through CD63 immunostaining (which showed that 98.8% of the isolated vesicles are CD63-positive). The MNs were divided into two groups: Treated (I) With doxycycline (Dox) in a concentration of 0.1 µg mL^{-1} (which represents the health control group) and (II) Without DOX (which represents the TDP43 mislocalization pathologies as seen in neurodegenerative disease like in ALS diseased MN). Both groups were divided into four subgroups: (I) No treated with hIDPSC-derived exosomes, treated with the exosomes at a concentration of (II) 25 µg mL^{-1}, (III) 50 µg mL^{-1} and (IV) 75 µg mL^{-1}. The cells were automatically imaged at low magnification (20X objective) by Incucyte Live-Cell Imaging and Analysis Instrument (Sartorius, Michigan, USA) at one, seven and 14 days *in vitro* (DIV). The images were automatically analyzed by Incucyte software (Sartorius, Michigan, USA) using the neurite tracking function to analyze the cell body cluster area (area/mm^2), cell body cluster count (per mm^2) and neurite length (mm/mm^2). All assays were performed in quintuplicate in 2 independent experiments.

Statistical analysis: Data were analyzed using nonsupervisioned machine learning (PCA), using k-means to cluster the cells according to their transcriptome and Kruskal-Wallis Test, followed by Dunn's *post hoc* Test, both with a significance level of 5%. Analyses were performed using R-4-3-0 software.

RESULTS

Overview of RNA-Seq: After to confirming that all analyzed samples showed a satisfactory sequencing quality (with a medium Phred score of 36, which indicates an accuracy higher than 99.9%, Table 1) the reads were aligned and mapped using the human reference genome. Results generated a total number of unique reads mapped to the human genome between 6.8 and 60.9 million, with a mean (Standard Deviation (SD)) across samples of 18.5 (9.9) million (Table 1). These reads were summarized into gene-level expression counts, resulting in a mean (SD) of 26.6 (8.0) successfully assigned reads for the NestaCell® product and 30.5 (18.0) million for the other 137 MSC samples (Table 1). The differences in the number of reads between NestaCell® product samples and other analyzed MSCs were not statistically significant (Student's t-test, p-valor = 0.8379). Count data as filtered. After filtering, 15,046 genes were analyzed for differential expression. The MDS plot (based on the gene-level expression counts of these 15,046 mapped genes) clearly distinguished the MSC populations, grouping samples from the same tissue origin in well-defined clusters, according to their transcriptional profile (Fig. 1a). The four sequenced batches of the active component of the NestaCell® product (hIDPSCs) grouped in unique cluster that, although it is dimensionally closer to AD-MSC samples, it does not overlap with any other MSC cluster. This result shows that the hIDPSCs, as well as the other MSCs, have a unique transcriptome profile that is related to the origin of these cells (Fig. 1a). Results also show that the hIDPSC samples are grouped among themselves with a less dimensional distance when compared to other MSC population, suggesting that the transcriptomic stability of these cells. Confirming these data, we also demonstrated that the MDS plot based on the gene-level expression counts of these 15,046 mapped genes, excluding the 375 genes uniquely expressed by the hIDPSCs modified its graphical profile, indicating that the remotion of these genes reorganizes the hIDPSCs to a single MSC cluster (Fig. 1b). These data suggest that these genes are important to molecularly segregate the active component of the NestaCell® product.

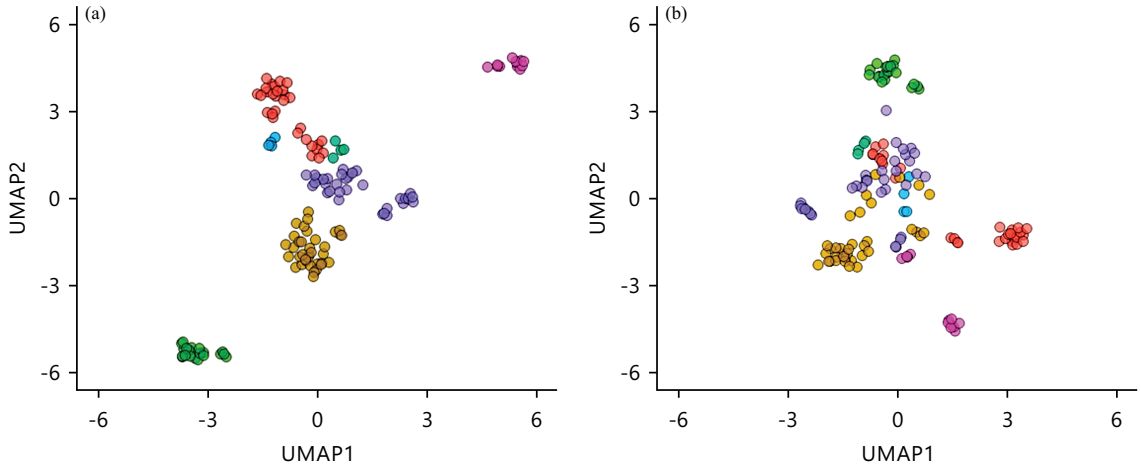

Fig. 1(a-b): Multidimensional scaling (MDS) plot based on the gene-level expression counts of these 15,046 mapped genes

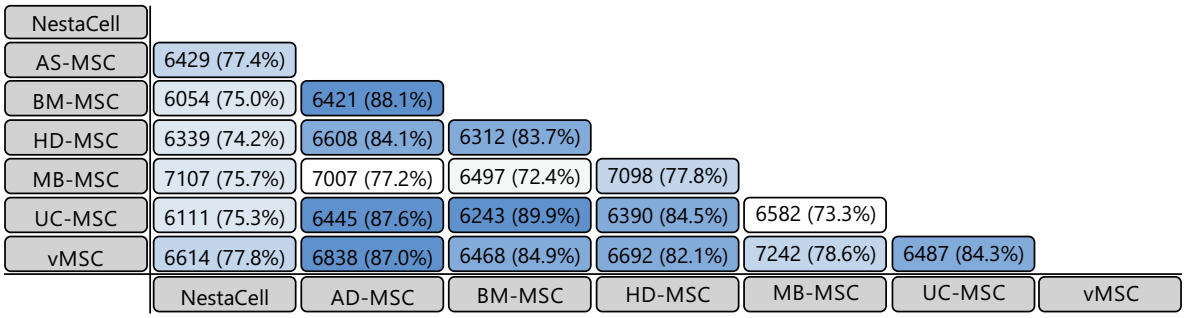

Fig. 2: Correlation matrix based on the transcriptomic profile of each MSC population, results show that all analyzed MSC populations share at least 72% of transcriptomic similarity

Analyses were performed using the UMAP technique (Fig. 1a-b). Interestingly, the MDS plot also showed that the hIDPSC samples (NestaCell® product) are grouped among themselves with a less dimensional distance when compared to other MSC populations (Fig. 1a), suggesting that the manufacturing process (under GMP) of the hIDPSCs ensures a high standardization and product stability. By contrast, we observed a long distance among the AD-MSC and UC-MSC samples (Fig. 1a), indicating a higher heterogeneity among the samples.

Active component of the hIDPSCs (NestaCell® product) has more than 70% of transcriptional similarity with other MSCs: The mean of gene-level expression counts was calculated among the samples derived from each tissue origin to identify the transcriptional profile of different MSC populations analyzed. Next, the genes with expression counts <10 were excluded to obtain a list of expressed genes that comprise the transcriptional profile of each MSC population (Table 2).

The lists containing the set genes comprising each MSC populations transcriptional profile were qualitatively compared to identify the genes commonly expressed by all MSC populations. In this analysis, 5,913 genes commonly expressed by all MSCs were identified, representing 72.74% of the genes expressed by the active component of the NestaCell® product (Table 3). This percentage is like the other six MSCs populations, which varies from 74.18% (vMSCs) to 85.53% (BM-MSCs) (Table 1). Altogether, these data reinforce that, despite the ectomesenchymal origin of the hIDPSCs, these cells can be classified as MSC-like. These results were confirmed by the transcriptomic correlation matrix, which shows that all MSC population analyzed share at least 72% of transcriptomic similarity (Fig. 2).

Table 2: Genes identified as uniquely expressed in the active component of the NestaCell® product

LRCH4	GPR173	ACBD4	EPM2A-DT	KCND1	ZNF792
LRCH2	CASC15	SHTN1	RPS6KA1	CAND2	SNORD99
IL18BP	LINC00342	CCDC191	NTF3	CCDC85C	KIAA1549
RGMB-AS1	SEC31B	SLC29A4	PTCH1	ZNF678	KIFC2
PDCD6	PSMB10	LCAT	IL15RA	AMER1	LHX8
TRMT9B	ST6GAL1	HID1	SNX22	GOLGA8A	TDRP
GSEC	ZNF546	RAB26	ZSCAN2	MRPL23	LINC00968
NEIL1	ALS2CL	MUC20-OT1	DISC1	PAX3	NOVA1
ANKMY1	HES4	BCL11A	MATR3	BATF3	P2RX6
NBPF11	ZNF8	GRAMD1C	PLXNC1	SNHG26	PNPLA3
ZNF213-AS1	GAL3ST4	FBXO41	SOCS2	ZNF737	DMKN
PRPF40B	TRMT61B	FAM228B	GAS7	CCDC7	GOLGA8B
CLEC2D	GALNT14	LINC00174	PLA2G6	CDHR3	VASH1
PCSK4	GSTO2	RNF112	TMEM178A	PRTG	TESMIN
ZNF865	GRTP1	KLHL17	ZNF525	EXPORT	WSCD1
C1orf159	TRIM66	CTSH	UBL4B	TCIM	MTSS1
NPEPL1	EIF4E3	RPL32P3	THBS4	TSNARE1	TTC28-AS1
STEAP1B	CYRIA	OSR2	RGL3	ZNF141	ANKRD33B
MIR222HG	NACAD	ANKDD1A	TMEM51	LTK	SNORA3B
CAPS	CENATAC	PRDM10	USP49	CLDN23	TVP23C
ARRB2	EGLN2	MMP11	RGS11	SEPTIN4	ACE
ZFPM1	TAMALIN	PATJ	DNHD1	WWC1	ITPKA
XRCC3	CCDC146	LINC00839	LINC00475	TFAP2A	ARVCF
GRIN3B	PPIEL	SPEF2	DZIP1L	LEF1	EBF4
RAPGEFL1	TAF4	SNORD104	GAS6-AS1	REC8	PROB1
SPACA6	SNHG10	LINC-PINT	MST1	BDNF-AS	CARMN
AZIN2	EYA2	ZNRF3	ZNF853	RUNX3	MAPK10
TJP2	FAM83H	SCIN	FHIP1A	NT5M	SOX9
GLI4	SHANK1	ATP1A1-AS1	FAHD2B	CLCA2	FOXF2
ANO8	EDARADD	DPF3	CELSR3	LZTS1	ACVR2B
KLHL3	APOBEC3F	MBNL1-AS1	ADSS1	HELLPAR	PRRT2
CCDC188	ZDHHC14	PYCARD	DNMT3B	LRRC75B	SIX2
C20orf96	HIC2	STAP2	TFAP4	RTL1	DNM1P47
SLC9A5	DPY19L2P1	NAGS	ABCC6	SOCS1	SALL1
SYCE1L	ATF7IP2	ZNF354B	SGCD	B4GALNT4	GDNF
MYO15B	STAR	CCDC152	ZNF710	NBEAL2	PLXNB3
TCF7L2	PABPC1L	LETM2	TMEM132B	POU2F2	SLC9A3-AS1
AGAP2-AS1	CYB5RL	DNAH5	PARD6G	WNT5A-AS1	ASPHD1
PLEKHG3	CFAP69	KATNAL2	SH3BP1	RPS15P4	C1orf115
ZNF483	CACNA1A	FSD1	MIR34AHG	GPR85	TRHDE-AS1
RPL13AP25	SATB2-AS1	MYPN	ANKAR	TFAP2C	BDH1
RNF207	BTBD8	LIF-AS2	KANTR	POU6F1	IGF2
IL11	CRABP2	SUZ12P1	SPIRE2	APOBEC3G	ADAMTS9-AS2
PKD1P6	EFCAB13	ZNF205	SCARF1	RFX3	FTLP3
CISH	PRDM11	PDE1C	NBEA	SALL2	SNORA33
LRCH4	SCNN1D	PRELID2	NRSN2-AS1	COL24A1	EPHA4
MARCHF9	TMEM158	OSBPL7	CDCA7	FOXQ1	PPARG
STARD13-AS	ROBO3	DIO3OS	FENDRR	SNAP25	CLMN
EGR3	ST6GALNAC5	IGDCC4	STMN3	XACT	COPB2-DT
TET1	BMF	PM20D2	PIK3C2B	DENND2A	PDE4DIPP2
RRAD	MYRF	LINC01515	VAT1L	CDKN1C	ETNK2
PLPPR3	SOX6	MIAT	PKD1L2	RNF157	NR4A3
ANKRD36	FER1L4	BCL2L11	ZNF804A	EYA1	ANKRD29
TRHDE	RAB38	IL16	MBOAT1	MSANTD2-AS1	DPY19L2
PSD	RASL11A	RAB3D	OBSCN	PAPLN	SDK1
SHANK2	MOV10L1	KIF5A	RASD1	APCDD1	MAFB
EVI2A	LRP5L	BAALC-AS1	SAMD5	RIPOR3	MSX2
CMYA5	GUCY1A2	PPL	TSPOAP1	RBP1	NPTX1
WNT7B	PLEKHA6	TUBB3	BCL2	ITPRIPL1	USP43
RASSF5	PCBP3	GATA3	FHOD3	RAB11FIP1	HCN2
GLIS1	SETBP1	PLIN4	ACACB	RGS17	
C1RL-AS1	SHF	ODF3B	ADRA1B	ACTG2	
SYTL2	EPHB6	SFMBT2	MKX	NR4A2	

Table 3: Number of expressed genes

MSC	Mapped genes	Mean of gene count >10[1]	Percentage of genes commonly expressed[2]
NestaCell®	15,046	8,128 (100%)	5,913/8,128 (72.74%)
AD-MSC	15,046	7,582 (100%)	5,913/7,582 (77.98%)
BM-MSC	15,046	6,913 (100%)	5,913/6,913 (85.53%)
UC-MSC	15,046	7,012 (100%)	5,913/7,012 (84.32%)
MB-MSC	15,046	9,594 (100%)	5,913/9,594 (61.63%)
HD-MSC	15,046	7,740 (100%)	5,913/7,740 (76.39%)
vMSC	15,046	7,971 (100%)	5,913/7,971 (74.18%)

[1]Total number of mapped genes with a mean of count >10 per MSC population (genes that comprise the transcriptional profile of each MSC population), [2]Relation (percentual) of the number of commonly expressed genes among the se seven MSC populations (5,913) and the number of expressed genes that comprise the transcriptional profile of each MSC population

Table 4: Percentual of transcriptional similarity of each MSC population with different human health tissues

MSC population	Liver	Kdiney	Lung	Bone marrow	Brain	Spleen
NestaCell®	85.06[a]	78.49[a]	76.89[a]	71.05[a]	68.42[b]	65.98[b]
AD-MSC	87.43[a]	76.58[a]	74.86[a]	72.44[a]	67.16[b]	61.09[b]
BM-MSC	86.06[a]	76.81[a]	73.98[a]	73.99[a]	67.31[b]	61.69[b]
HD-MSC	84.90[a]	75.07[a]	73.58[a]	71.85[a]	65.70[b]	60.57[b]
MB-MSC	85.81[a]	75.42[a]	73.31[a]	71.92[a]	65.65[b]	59.67[b]
UC-MSC	86.20[a]	76.45[a]	73.80[a]	72.91[a]	64.32[b]	59.45[b]
vMSC	86.02[a]	76.75[a]	74.23[a]	72.16[a]	65.37[b]	60.19[b]
Mean	85.92	76.51	74.37	72.33	66.27	61.23

Values followed by equal letters indicate the absence of significant statistical differences (p-value>0.05). Values followed by different letters indicate significant statistical differences (p-valor<0.05). Statistical analysis was performed through two-way ANOVA (p-value = 0.0021), followed by the Bonferroni *post-hoc* test. AD-MSC: Adipocyte-derived mesenchymal stem cells, BM-MSC: Bone marrow mesenchymal stem cells, MB-MSC: Menstrual blood mesenchymal stem cells, UC-MSC: Unbilical cord mesenchymal stem cells, HD-MSC: Hepatocyte-derived mesenchymal stem cells and vMSC: Vertebral mesenchyma stem cells

Based on these data, we compare the transcriptome profile of the seven MSC populations with the transcriptome of different healthy human tissues using the database available in the FunRich software. Results showed that all analyzed MSC samples share a high transcriptional similarity with human health liver (mean 85.92%), kidney (mean 76.51%), lungs (mean 74.37%), bone marrow (72.33%), brain (mean 66.27%) and spleen (61.23%) (Table 4). However, there were no verified significant statistical differences between the MSC populations (Table 4), which was by the high transcriptional similarity (higher than 72%, Table 3) among these cell populations.

The transcriptional profile from the seven MSC analyzed populations with the transcriptome of different brain areas was also compared. The analyzed MSC populations share transcriptional similarities with the cerebellum and hippocampus (mean 58.10 and 57.74%, respectively, Table 5). However, as verified for the comparative analysis with other human health tissues, no statistical differences among the percentage of transcriptional similarity in the MSC populations were verified (Table 5).

Active component of the hIDPSCs (NestaCell® product) expresses unique genes that regulate metabolic processes and neurogenesis: Aiming to analyze the biological process regulated by the genes expressed by the seven studied MSC populations, the transcriptome of these cells was subjected to functional enrichment analysis using the FunRich software. Results showed that the active component of the NestaCell® product expresses about 2-fold more genes involved in cell communication and signal transduction when compared with the transcriptome of other MSC populations (Fig. 3), suggesting that the hIDPSCs possess a greater capability of interacting with recipient cells.

Additionally, we identified 375 genes that are uniquely expressed in the active component of the NestaCell® product (Table 2). These genes represent 4.61% (375/8,128 genes) of the transcriptome of the hIDPSCs.

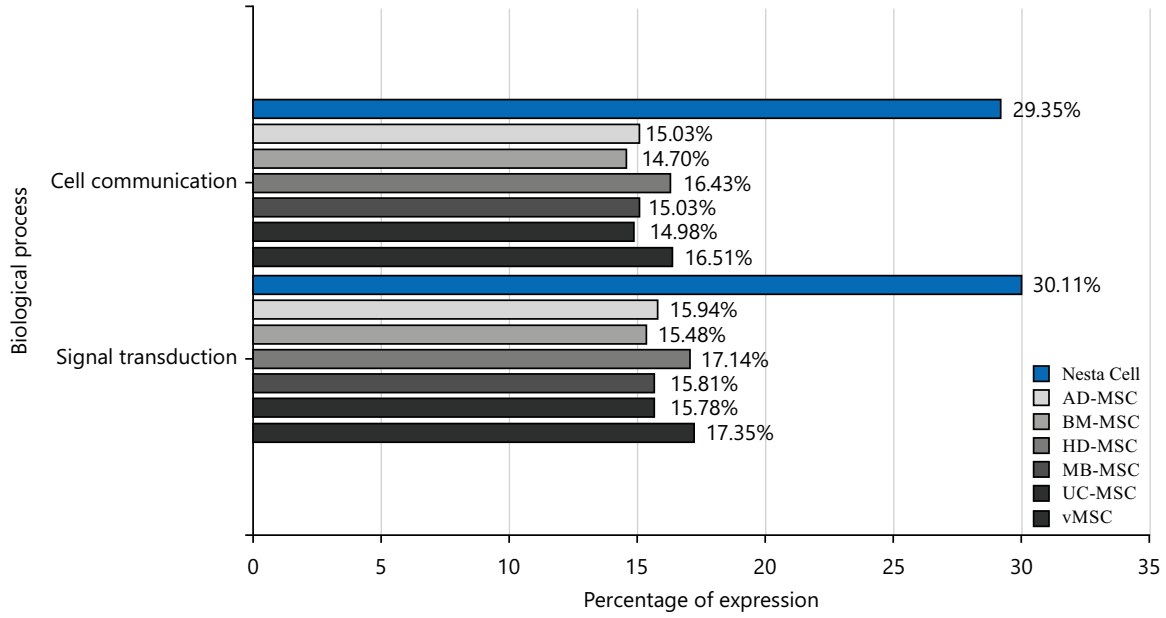

Fig. 3: Functional enrichment analysis based on the biological process showing the active component of the NestaCell® product (hIDPSCs) naturally express about 2-fold more transcripts involved in cell communication and signal transduction in relation to other MSCs. Analysis was performed using the FunRich software

Table 5: Percentual of transcriptional similarity of each MSC population with different human health brain areas

MSC	CB	HC	Liquor	Cortex	SN	Amygdala
NestaCell®	63.26^{a}	46.77^{a}	30.87^{b}	10.99^{c}	5.00^{d}	5.07^{d}
AD-MSC	58.14^{a}	58.19^{a}	27.48^{b}	14.94^{c}	4.98^{d}	4.95^{d}
BM-MSC	58.56^{a}	58.50^{a}	28.97^{b}	16.81^{c}	4.83^{d}	4.87^{d}
HD-MSC	53.33^{a}	56.25^{a}	23.15^{b}	14.61^{c}	4.96^{d}	4.91^{d}
MB-MSC	57.10^{a}	57.25^{a}	25.91^{b}	15.50^{c}	4.92^{d}	4.94^{d}
UC-MSC	57.80^{a}	57.74^{a}	27.97^{b}	15.62^{c}	4.90^{d}	4.92^{d}
vMSC	58.55^{a}	58.40^{a}	26.48^{b}	15.40^{c}	5.56^{d}	5.54^{d}
Mean	58.10	57.74	27.26	14.83	5.02	5.02

Values followed by equal letters indicate absence of significative statistical differences (p-valor>0.05). Values followed by different letters indicate significative statistical differences (p-valor<0.05). Statistical analysis performed through two-way ANOVA (p-valor = 0.0001), followed by the Bonferroni *post-hoc* test. CB: Cerebellum, HC: Hippocampus, SN: *Substantia nigra*, AD: MSC-adipocyte-derived mesenchymal stem cells, BM-MSC: Bone marrow mesenchymal stem cells, MB-MSC: Menstrual blood mesenchymal stem cells, UC-MSC: Unbilical cord mesenchymal stem cells, HD-MSC: Hepatocyte-derived mesenchymal stem cells and vMSC: Vertebral mesenchyma stem cells

To verify the importance of these genes for the transcriptomic signature of the active component of the NestaCell® product, a novel MDS plot excluding these 375 genes of the hIDPSCs transcriptome was performed. Interestingly, the results of these exploratory analyses showed that the remotion of the genes uniquely expressed by the hIDPSCs alters the changed graphical profile of the MSCs, clustering the active component of the NestaCell® product with other MSCs (Fig. 1b). This data provide evidence that these 375 genes comprise the transcriptomic signature of the hIDPSCs and make these cells unique for therapeutic applications. Additionally, the hIDPSCs have about 60% of the genes overexpressed by the active component of the NestaCell® product are also overexpressed by AD-MSCs (Fig. 4a), BM-MSCs (Fig. 4b), HD-MSCs (Fig. 4c), UC-MSCs (Fig. 4e) and vMSCs (Fig. 4f), except by the MB-MSC (about 15%, Fig. 4d). Enrichment analysis by over-representation (ORA) showed that: (I) 174 of these uniquely expressed genes regulate the metabolic process, (II) 115 genes are involved in the cell communication process, (III) 51 genes are involved in neurogenesis, (IV) 13 genes are enrolled in neuron to neuron synapse, (V) 10 genes are expressed in both neuron and dendritic spine and (VI) 8 genes are associated with axon guidance (Table 6).

Active component of the hIDPSCs (NestaCell® product) overexpress mitochondrial genes involved in energy metabolism: Based on the thresholds set for log2FC and p-value, comparing the genes commonly expressed by the seven MSC populations, we identified 75 genes that are overexpressed in the active component of the NestaCell® product (log2FC>1, Table 6. Although all MSCs analyzed share at least 72% of transcriptomic similarity among them (Fig. 2), we observed that, in quantitative terms, the MB-MSC comprises the MSC population with the fewest number of overexpressed genes (log2FC>0.5 or $2^{0.5}$ = 1.41-fold (Fig. 4). Interestingly, among these genes, we observed that the mitochondrial genes

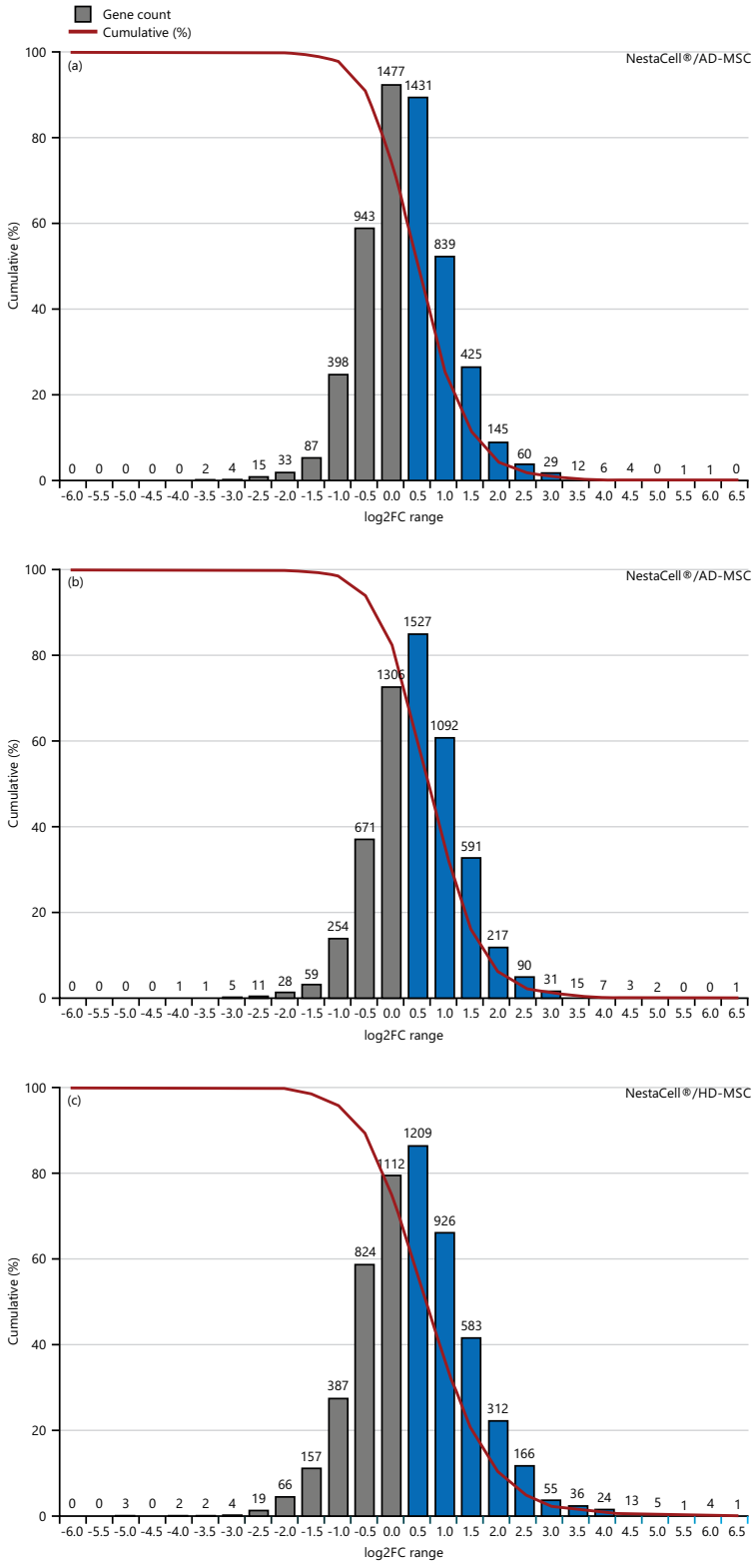

Fig. 4(a-f): Continue

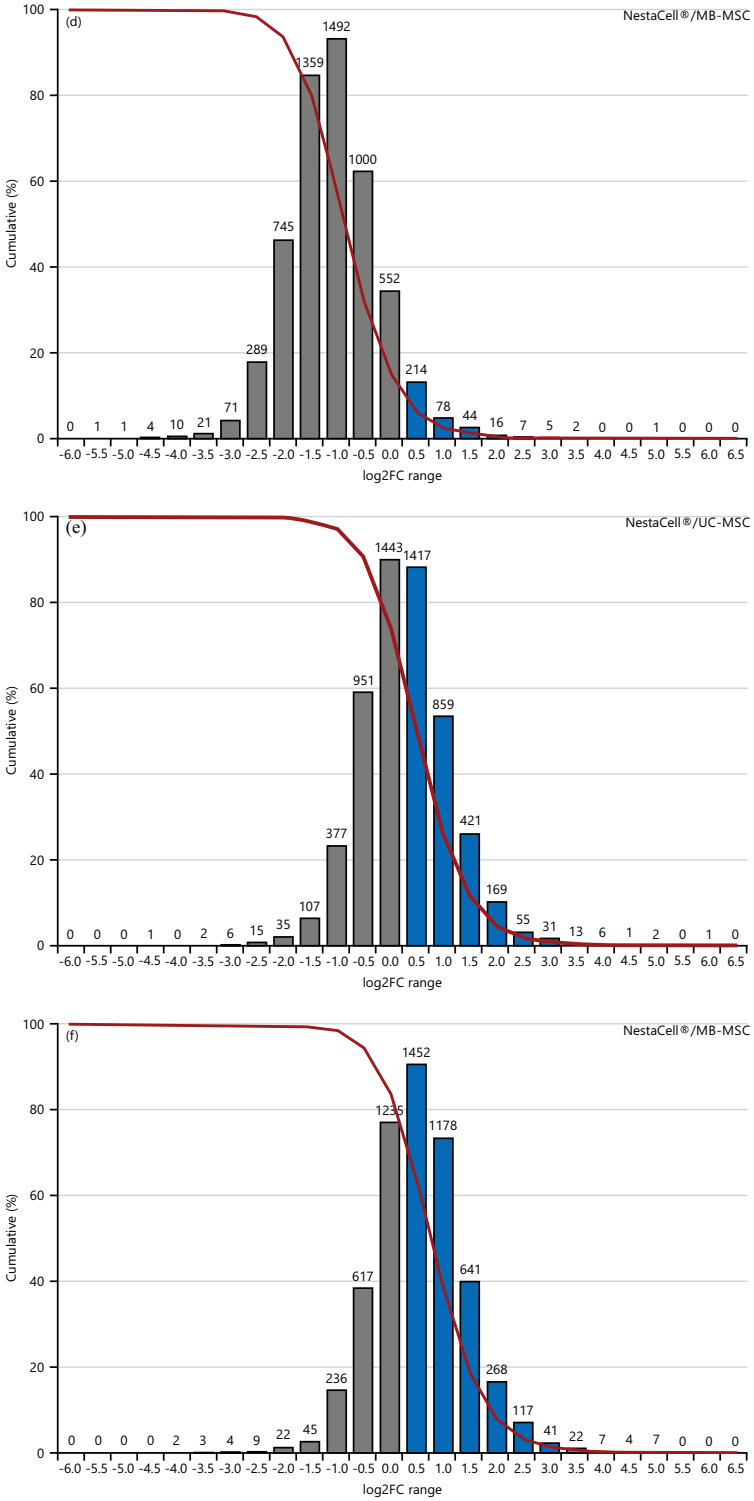

Fig. 4(a-f): Histograms showing the log2FC ratio between the genes commonly expressed by the active component of the NestaCell® product and other MSC populations. Results describe the number of genes (bars), including those genes that are overexpressed (log2FC >0.5, bars in blue) and the cumulative percentage of these genes (red line). Results show that about 60% of the genes overexpressed by the active component of the NestaCell® product are also overexpressed by (a) AD-MSCs, (b) BM-MSCs, (c) HD-MSCs, (e) UC-MSCs and (f) vMSCs, except by the MB-MSC (about 15%, D)

AD-MSC: Adipocyte-derived mesenchymal stem cells, BM-MSC: Bone marrow mesenchymal stem cells, MB-MSC: Menstrual blood mesenchymal stem cells, UC-MSC: Unbilical cord mesenchymal stem cells, HD-MSC: Hepatocyte-derived mesenchymal stem cells and vMSC: Vertebral mesenchyma stem cells

Table 6: Results of the enrichment analysis of the 375 uniquely expressed genes identified in the active component of the NestaCell® product

Enrichment to	Gene set	FDR	p-value	Overlap
Neurogenesis[1]	GO:0022008	0.0001	0.0000	51
Neuron spine[2]	GO:0044309	0.0078	0.0000	10
Dendritic spine[2]	GO:0043197	0.0000	0.0078	10
Neuron to neuron symapse[2]	GO:0098984	0.0197	0.0000	13
Axon guidance[3]	hsa04360	0.6194	0.0041	8

[1]Over-representation analysis (ORA), using gene ontology (GO) database for biological process, [2]Over-representation analysis (ORA), using geneontology (GO) database for cellular components, [3]Over-representation analysis (ORA), using the KEGG database for biological pathways, [4]Over-representation analysis (ORA), using PANTHER database for biological pathways and FDR: False discovery ratio

Table 7: Ordinated list of the 75 genes identified as overexpressed in the active component of the NestaCell® product

Gene	NestaCell®	AD-MSC	BM-MSC	UC-MSC	MB-MSC	HD-MSC	vMSC
MT-RNR2	28401.8	1818.7	1600.5	1967.5	4734.5	1266.2	1048.1
MT-CO1	22642.0	3364.1	3112.6	3137.6	8108.5	1778.3	2655.6
MT-RNR1	16825.3	265.0	193.8	263.6	657.8	186.0	162.5
MT-CO2	10746.3	1273.0	1079.8	1290.6	3285.0	633.0	1008.1
MT-CO3	10481.8	1442.7	1276.6	1673.9	3902.5	843.7	1428.7
MT-ND4	10172.3	1458.6	1387.7	1790.2	4506.8	806.7	1530.2
MME	8081.0	447.2	519.7	2672.0	1426.0	145.8	47.4
IGF2R	6954.5	410.3	348.3	430.6	1119.5	838.8	225.9
MALAT1	5931.5	990.3	999.8	732.1	2441.8	454.9	655.0
MT-ND1	5040.5	538.6	492.8	684.9	1694.3	364.5	633.1
PLEC	4738.0	747.1	895.7	798.6	1911.3	508.0	773.8
MT-ATP6	4054.0	565.0	528.6	744.1	1821.8	284.6	544.0
MT-ND3	2658.8	223.0	181.0	193.3	526.3	109.4	162.8
MT-ND4L	2408.5	182.6	168.8	221.1	560.5	102.1	203.7
SREBF2	2382.5	116.4	107.2	100.6	305.3	134.4	96.7
LPAR1	2310.5	221.3	189.3	211.2	532.0	126.6	241.7
MAP1B	2149.0	459.6	403.4	408.2	1057.8	428.5	299.6
NEAT1	1981.3	403.8	344.9	212.2	856.0	108.2	253.3
EGR1	1881.8	557.6	385.8	248.4	769.8	19.4	70.6
MDK	1770.3	46.8	72.1	72.2	182.3	38.6	76.5
MEG3	1465.3	178.1	137.2	267.2	423.0	148.4	121.1
ZFP36	1397.0	241.3	131.7	109.5	342.3	33.3	46.7
TNS3	1363.5	89.3	184.6	142.9	406.0	77.1	233.7
SOCS3	1248.0	166.7	142.8	108.1	288.0	39.8	129.4
ZEB1	1081.8	139.3	118.9	148.5	316.0	64.5	105.3
KANK2	1003.0	284.2	178.6	187.4	487.5	44.6	201.1
CEBPD	983.5	146.1	141.4	163.0	401.3	90.1	107.8
TBX3	964.0	55.4	31.9	67.7	113.5	16.7	43.3
JUNB	950.8	298.7	193.9	157.1	428.3	58.9	85.9
ACIN1	931.0	133.0	109.2	121.7	299.5	72.3	106.1
PSD3	924.0	111.5	181.3	158.6	406.3	75.3	122.8
ADM	765.0	200.9	147.1	112.9	344.5	32.2	70.5
TRAK2	759.0	100.2	92.2	84.1	232.0	83.6	79.0
NOP53	711.8	178.6	126.1	140.1	337.5	89.5	92.7
NFKBIZ	612.3	162.3	128.9	97.0	268.3	82.2	24.8
NUMA1	605.0	124.2	104.0	117.2	279.5	82.7	103.3
PDE5A	590.5	42.1	81.4	61.7	205.3	84.9	105.1
RAB12	505.5	39.8	39.3	37.5	89.0	44.1	31.8
ANP32B	503.0	83.6	69.3	91.0	203.5	48.6	69.3
PTPRS	481.0	123.7	96.8	85.8	238.8	44.8	84.5
PARP14	477.8	84.6	71.8	81.5	238.8	117.0	68.0
RBM25	468.8	77.4	79.2	81.2	199.5	41.9	87.3
RFLNB	468.3	46.4	38.7	68.1	155.5	93.2	45.9
NECTIN3	448.5	63.2	66.3	96.1	221.0	110.7	65.0
SOX4	412.8	63.2	86.4	69.6	198.8	16.0	136.8
PIM1	412.3	78.2	40.4	44.1	89.0	18.6	25.6

Table 7: Continue

Gene	NestaCell®	AD-MSC	BM-MSC	UC-MSC	MB-MSC	HD-MSC	vMSC
GNL2	401.5	53.4	56.4	58.8	142.5	60.7	46.4
GPSM1	375.8	40.2	52.8	51.3	117.8	32.9	66.3
CRAT	342.0	79.9	52.9	58.9	151.8	32.9	60.2
EVC	311.0	69.3	49.1	65.1	141.3	30.5	58.3
ALDH3B1	294.8	45.2	45.0	60.1	131.0	38.6	49.4
PLEKHA5	289.5	36.9	33.7	39.8	96.3	20.1	59.8
STARD13	288.5	38.2	53.6	45.5	118.5	13.2	66.5
FYCO1	285.3	51.6	47.8	49.1	115.8	27.3	70.0
MTCL1	285.3	32.3	31.8	34.1	85.3	28.5	19.0
PDE4D	282.8	35.8	40.1	72.9	124.8	33.5	89.6
TBX2	280.5	33.7	43.6	52.3	99.5	23.2	37.3
CHD6	278.8	53.0	51.7	53.7	132.0	34.1	55.4
CEP250	268.5	29.7	44.9	30.3	84.5	18.2	31.6
MAPK8IP3	268.0	46.4	53.2	45.5	105.8	20.0	50.3
NINJ1	266.0	36.6	28.6	43.7	99.0	41.3	33.8
MIDEAS	249.5	48.3	40.6	42.7	108.0	28.9	40.7
NOTCH1	244.5	25.0	22.1	27.6	62.8	48.5	11.9
AKAP17A	214.5	42.2	35.9	40.5	93.0	39.2	24.0
CCDC14	206.0	36.4	40.3	36.2	100.0	16.2	42.6
ZNF335	201.8	20.5	15.7	20.5	47.5	15.1	17.4
RGS10	193.5	40.9	34.0	30.5	77.5	14.4	20.9
RREB1	190.5	43.8	32.0	35.3	91.8	32.1	23.8
KAT6B	181.3	35.1	29.9	33.3	83.0	18.1	30.2
GIGYF1	181.0	42.5	32.3	34.8	87.0	27.4	28.2
ZFHX3	180.3	25.5	28.5	30.6	74.5	16.5	43.2
FAM118A	178.8	25.7	26.7	22.9	58.8	15.1	14.3
FIP1L1	165.8	22.2	18.6	22.3	56.3	27.2	15.8
EFNB1	165.3	44.9	41.5	32.3	75.3	27.9	28.4
TMEM132A	158.5	24.0	26.3	61.6	79.0	44.6	20.1

AD-MSC: Adipocyte-derived mesenchymal stem cells, BM-MSC: Bone marrow mesenchymal stem cells, MB-MSC: Menstrual blood mesenchymal stem cells, UC-MSC: Unbilical cord mesenchymal stem cells, HD-MSC: Hepatocyte-derived mesenchymal stem cells and vMSC: Vertebral mesenchyma stem cells

Table 8: Functional enrichment analysis of the 75 genes overexpressed by the active component of the NestaCell® product

Enrichment to	Gene set	FDR	p-value	Overlap
Developmental process[1]	GO:0051094	0.0110	0.0000	17
Oxidative phosphorylation[2]	hsa00190	0.0097	0.0000	6
ATP synthesis[1]	GO:0042775	0.0047	0.0000	6
Respiratory chain complex[2]	GO:0098803	0.0002	0.0000	6
Respiratory chain complex IV[2]	GO:0005751	0.0033	0.0000	3
Parkinson's disease[3]	hsa05012	0.0097	0.0000	6

[1]Over-representation analysis (ORA), using geneontology (GO) database for biological, [2]Over-representation analysis (ORA), geneontology (GO) database for cellular components, [3]Over-representation analysis (ORA), using the KEGG database for biological pathways, Over-representation analysis (ORA), using PANTHER database for biological pathway, 3.5 active component of the hIDPSCs (NestaCell® product) promotes axon guidance through exosome-mediated mechanisms

MT-RNR2, *MT-CO1*, *MT-RNR1*, *MT-CO2*, *MT-CO3* and *MT-ND4* are the most expressed genes by the active component of the NestaCell® product (Table 7), reinforcing that the NestaCell® product can promote metabolic energy regulation, as previously observed in the enrichment analysis of the 375 genes exclusively expressed by the hIDPSCs (Fig. 4).

Confirming this result, functional enrichment analysis of the 75 genes overexpressed by the hIDPSCs showed that six genes codify proteins of mitochondria complex I, regulating oxidative phosphorylation and ATP synthesis. For this reason, it does not surprise that some of these genes were identified as downregulated in PD, reinforcing the therapeutic potential of the NestaCell® product for the treatment of neurodegenerative disorders, including ALS. Function enrichment also showed that 17 of these 75 overexpressed genes are involved in the developmental process, particularly with neurogenesis (Table 8).

Based on the functional enrichment analyses results, which suggest that eight of the 375 genes uniquely expressed by the active component of the NestaCell® product are involved in the regulation of axon guidance and growth. Thus, we treated primary motor neurons (MNs) from transgenic NEFH-hTDP-43ΔNLS mice with three different concentrations of hIDPSC-derived exosomes. Results showed no statistical difference for neurite length, cell body area and cell body cluster among the MNs treated with DOX and exosomes along the analyzed times (Fig. 5a-i), as expected. However, we observed that the exosomal treatment in MN cultures without DOX promoted the neurite length growth

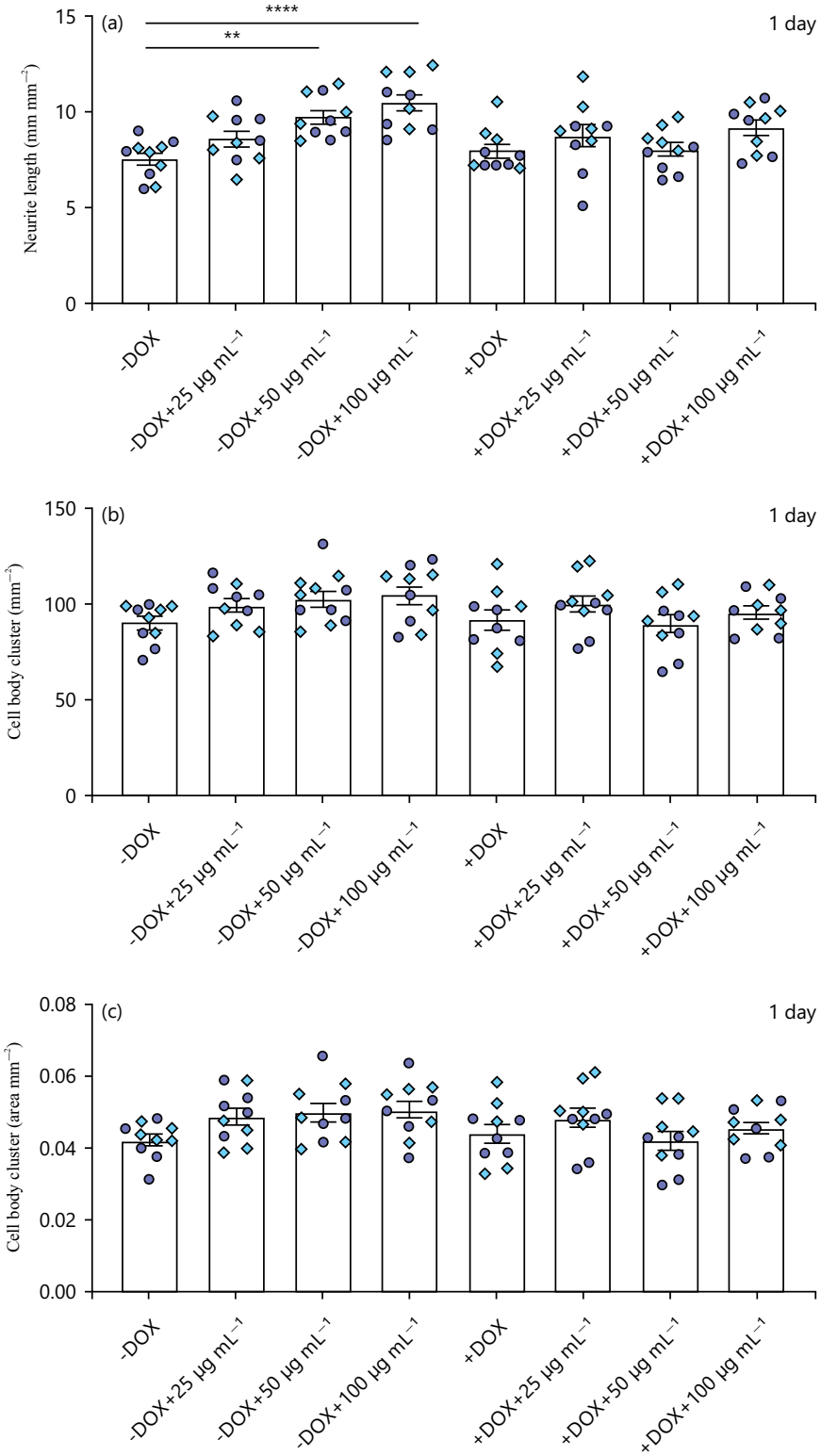

Fig. 5(a-i): Continue

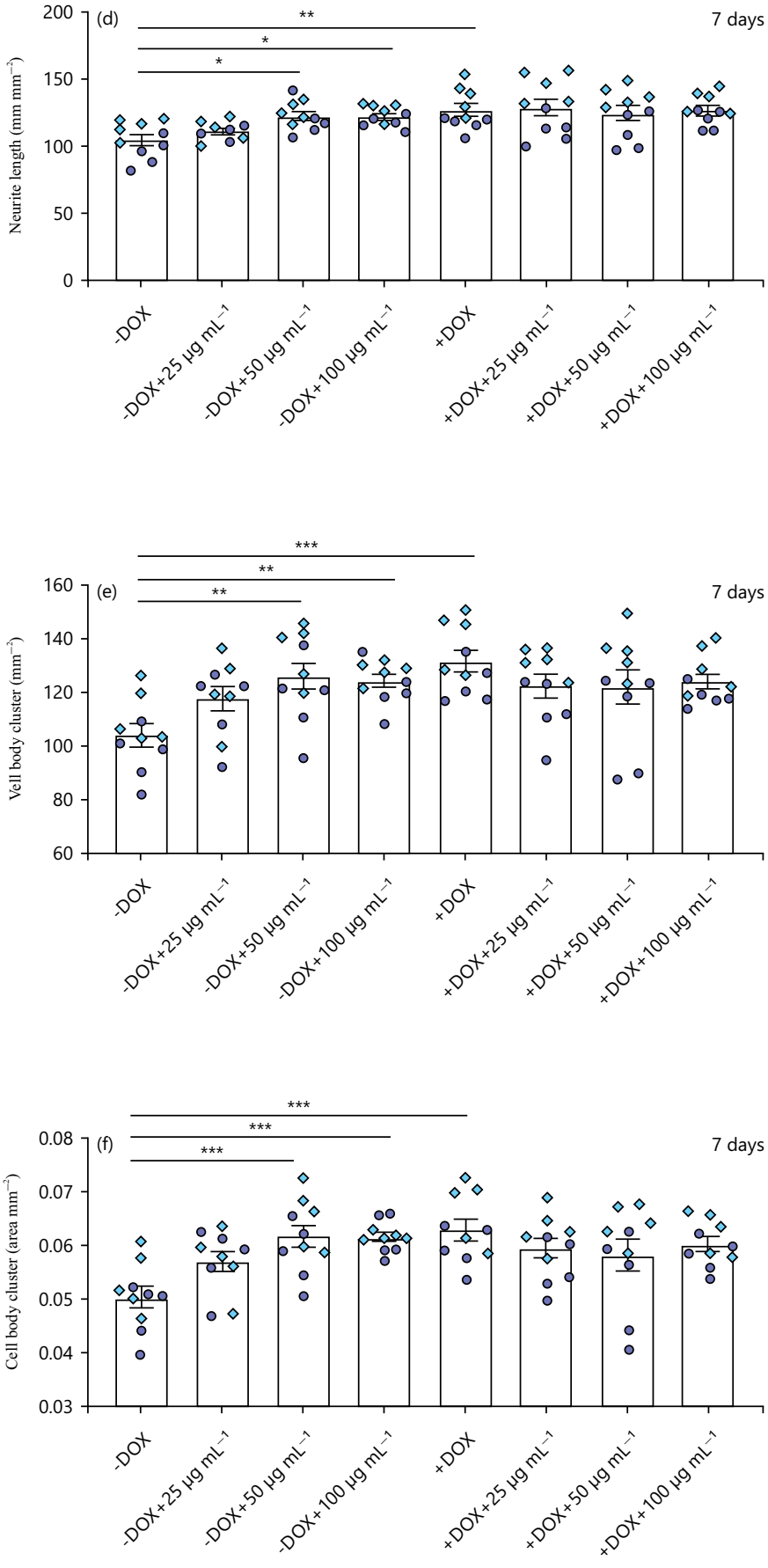

Fig. 5(a-i): Continue

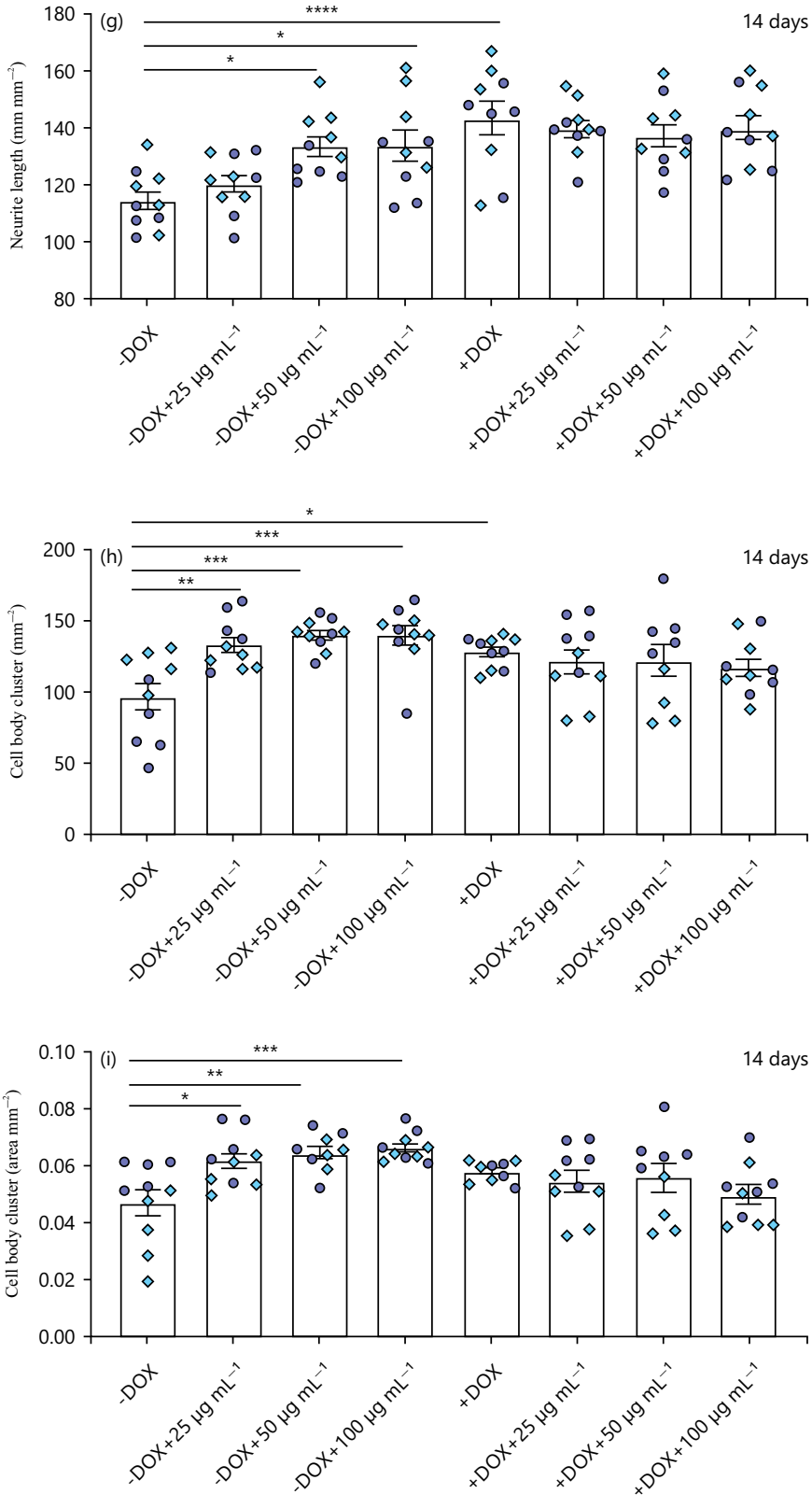

Fig. 5(a-i): Result of *in vitro* assay to assess the axon guidance. Results show that the treatment with hIDPSC-derived exosomes increased the neurite length in MNs cultivated without DOX in a concentration-dependent manner from 24 hrs (1 day, (a)) and in a time-dependent manner (7 and 14 days, (d and g), respectively). Similar results were observed from the 7 days to cell body cluster (b-h) and area (c-i)

*p-valor<0.05, **<0.001 and ***<0.0001. Assays were performed in quintuplicate in two independent experiments (circles in light and dark blue)

(from 24 hrs of analysis, Fig. 5a, d and g), cell body area (Fig. 5b, d, e and h) and cluster (from 7 days of analysis, Fig. 5c, f and i) in an exosome concentration-dependent manner (Fig. 5). Although these results do not confirm the RNA-Seq results, but also provide *in vitro* evidence that the axon growth and guidance-related genes produced by the active component of the NestaCell® product can be delivered to recipient neurons through naturally produced and secreted exosomes by hIDPSCs.

DISCUSSION

Because of their complex pathophysiology, which involves deregulations in multiple biochemical pathways, including mitochondrial dysfunctions, pharmacological treatment of neurodegenerative disorders offers limited therapeutic benefits. This is large because drugs act specifically on in one or a few targets. In this sense, advanced cellular therapy products emerge as a potential candidate for treating these diseases, since their active component (therapeutic cells) expresses and produces a plethora of bioactive molecules able to act in multiple targets simultaneously, offering broader therapeutic benefits than conventional drugs.

In this context, the Human Immature Dental Pulp Stem Cells (hIDPSCs) comprise a particular type of therapeutic cells, especially for treating neurodegenerative disorders. This is because, due to their ectomesenchymal origin (from neural crest), these cells naturally express genes that are constitutively expressed by the Central Nervous System (CNS), as revised by us[1,3,38]. For this reason, we have investigated the therapeutic potential of these cells for the treatment of different diseases[29,39,40], including HD[14,20] and PK[28]. Although we had provided clinical evidence that these (which comprise the active component of the NestaCell® product) are safe and can improve motor function for patients with HD (ClinicalTrial.gov identifiers NCT02728115, NCT03252535, NCT04219241)[41], the mechanism of action of these therapeutic cells remains not entirely understood.

In preclinical studies, we demonstrated that the intravenous treatment with the NestaCell® product was able to restore the cortical expression of BDNF (Brain-Derived Neurotrophic Factor) (which in HD is downregulated by mutated huntingtin protein) in rats subjected to the treatment with 3-NP (animal model for HD)[42-44]. The BDNF renders trophic and protective actions on striatal DARPP32-conatining neurons[45], while D2R is involved in DARPP32 modulation[46]. Thus, we also observed the expression of DARPP32 and D2R within the striatum of rats treated with 3-NP. This study provided evidence that the active component of the NestaCell® product has neuroprotective and neuro regenerative properties[14,20]. These results also suggest that these therapeutic properties are conferred by the natural capability of the hIDPSCs to express and secrete BDNF (striatal neuron survival-related neurotrophic factor which is downregulated in patients with HD[47]) that, when overexpressed, can prevent loss and atrophy of striatal neurons, improving motor function[48,49]. However, currently, we demonstrated that the intravenous transplantation of the NestaCell® product in rats intrastriatally treated with 6-OHDA (an animal model for PK) recovered the motor, cognitive and neuropsychiatric functions only three days after the product administration[28], suggesting that the active component of the NestaCell® has additional MoA, as expected for a CTP. For this reason, herein we perform a comparative analysis of the transcriptome of the hIDPSCs with other MSCs to identify the transcriptional signature of the active component of the NestaCell® product and, therefore, predict possible MoA which could justify the therapeutic response verified in both preclinical and clinical studies.

Using the RNA-Seq, we identified that the active component of the NestaCell® product expresses 375 unique genes (which are not expressed by any other MSC population analyzed) and overexpresses 75 genes from 5,913 genes commonly expressed by the other six MSC populations analyzed. Combined, these 450 differentially expressed genes comprise the transcriptional signature of the active component of the NestaCell® product. Functional enrichment analysis revealed that 51 of the 375 genes exclusively expressed by the hIDPSCs are involved in neurogenesis regulation. This result suggests that these 51 genes exclusively expressed by the active component of the NestaCell® product, can cooperate with the BDNF leading to the neuroprotection and neuro regeneration observed in the preclinical study for

HD[14,20]. Besides this, the enrichment analysis showed that 13 of these 375 genes are related to neuron-to-neuron synapses and eight of them, which axon guidance. These results are by the neuroprotective action of the NestaCell® product verified in our preclinical study for HD[4,21] and with the motor function improvements observed in both patients with HD treated with NestaCell®[42] and in the preclinical study for PD[28]. This is because accumulating evidence has shown that synaptic impairments and axonal degeneration precede neuronal cell body loss[49-51]. This hypothesis was by accumulating evidence that the MSC therapeutic properties are mediated by bioactive molecules (including mRNAs) naturally produced and secreted by these cells within extracellular vesicles[1,3,52,53].

Confirming this hypothesis, results showed that the treatment of primary motor neurons (MNs) from TDP43ΔNLS mice (an animal model for ALS) with exosomes isolated from the conditioned culture medium of the NestaCell® product promoted neurite length and growth in the cell body area and cluster in a dose-dependent manner, confirming the RNA-Seq results. These data also provide *in vitro* evidence that these differentially expressed transcripts can be delivered to recipient neurons through exosomes naturally produced and secreted by the hIDPSCs. This result suggests that these transcripts cooperate with the BDNF, conferring neurorregenerative and neuroprotective actions, justifying the therapeutic benefits observed in our preclinical[14,20] and Phase I clinical trial of the NestaCell® product for Huntington's disease[42].

Furthermore, the functional enrichment analysis showed that the active component of the NestaCell® product overexpressed mitochondrial genes, including *MT-RNR2*, which was found to be about 22-fold more expressed in the hIDPSCs than in other MSC populations. This gene encodes the human protein (HN), which is recognized to protect against neuronal death through intra- e extracellular mechanism[54], mediating neuroprotective effects by interacting with a receptor complex composed of IL6ST, IL27RA and CNTFR)[55] or acting as a ligand for G-protein coupled receptor FPR2/FPRL1 and FPR3/FPRL2[56]. In addition, studies showed that HN also suppresses the release of apoptogenic proteins from mitochondria by binding to BID[56,57-60], as well as reduces the superoxide production, reducing oxidative stress[61]. Considering that oxidative stress is the main responsible for neuro inflammation-mediated neuronal death, as revised by Teleanu *et al.*[62], these results suggest that the NestaCell® product can reduce neuro inflammation. This action can justify the motor, cognitive and neuropsychiatric improvements observed only three days after the intravenous administration of the NestaCell® product in animal models for PD[28].

Reinforcing this action, the active component of the NestaCell® product naturally overexpresses mitochondrial genes encoding different subunits of NADH dehydrogenase (*MT-ND1*, *MT-ND3* and *MT-ND4L*) were also verified, which form the respiratory chain complex I, which is mainly affected by the accumulation of neurodegenerative disorders-related misfolded proteins and, the main responsible for the superoxide production in neurodegenerative disorders. These results suggested that the NestaCell® product can improve mitochondrial function, decreasing oxidative stress and, therefore, neuro inflammation.

CONCLUSION

It is generally accepted that dental pulp stem cells originated from the embryonic neural crest However, a fair question may arise about their occurrence due to circulating adult stem cells mobilized from the bone marrow. This study demonstrated the difference in transcriptomic signature between BM-MSC and hIPDSCs and multiple genes expressed by hIDPSCs involved in neurogenesis, supporting our previous findings about the origin of hIDPSCs. Evidence were provided that the hIDPSCs (NestaCell® product) have a unique transcriptional signature, characterized by the differential expression of genes that promote axon growth and guidance. These properties combined with the secretion of BDNF (naturally produced by these cells) suggest that the NestaCell® product has neuro regenerative and neuroprotective actions, justifying the therapeutic effects observed by us in both preclinical and clinical studies for neurodegenerative disorders.

SIGNIFICANCE STATEMENT

Mesenchymal stem/stroma cells (MSCs) is a type of therapeutic cell that have been investigated for more than 30 years to treat noncurable diseases, including Alzheimer's, Parkinson's and Huntington's disease (neurological disorders). The MSCs can be obtained from different tissues, including teeth. However, the therapeutic capability of changes cells changes according to the tissue from which the cells were obtained. For this, this study aimed to compare the therapeutic capability of MSCs obtained from teeth with MSCs obtained from other tissues to identify the therapeutic properties of the cells isolated from teeth. Results obtained in this study showed that MSCs obtained from teeth have unique properties that can help to treat neurological disorders.

ACKNOWLEDGMENTS

The authors thank the Butantan Foundation and Cellavita Scientific Research Ltda., for the financial support.

REFERENCES

1. Kerkis, I., R.P. Araldi, C.V. Wenceslau and T.B. Mendes, 2022. Advances in Cellular and Cell-Free Therapy Medicinal Products for Huntington Disease Treatment. In: From Pathophysiology to Treatment of Huntington's Disease, Szejko, N. (Ed.), IntechOpen, London, UK, ISBN: 978-1-80355-427-3.
2. Muthu, S., M. Jeyaraman, M.B. Kotner, N. Jeyaraman and R.L. Rajendran *et al*., 2022. Evolution of mesenchymal stem cell therapy as an advanced therapeutic medicinal product (ATMP)-An Indian perspective. Bioengineering, Vol. 9. 10.3390/bioengineering9030111.
3. Araldi, R.P., F. D'Amelio, H. Vigerelli, T.C. de Melo and I. Kerkis, 2020. Stem cell-derived exosomes as therapeutic approach for neurodegenerative disorders: From biology to biotechnology. Cells, Vol. 9. 10.3390/cells9122663.
4. Vu, Q., K. Xie, M. Eckert, W. Zhao and S.C. Cramer, 2014. Meta-analysis of preclinical studies of mesenchymal stromal cells for ischemic stroke. Neurology, 82: 1277-1286.
5. Zhou, Q., M. Yuan, W. Qiu, W. Cao and R. Xu, 2021. Preclinical studies of mesenchymal stem cells transplantation in amyotrophic lateral sclerosis: A systemic review and metaanalysis. Neurol. Sci., 42: 3637-3646.
6. Sun, X.Y., X.F. Ding, H.Y. Liang, X.J. Zhang and S.H. Liu *et al*., 2020. Efficacy of mesenchymal stem cell therapy for sepsis: A meta-analysis of preclinical studies. Stem Cell Res. Ther., Vol. 11. 10.1186/s13287-020-01730-7.
7. Li, X., H. Wen, J. Lv, B. Luan and J. Meng *et al*., 2022. Therapeutic efficacy of mesenchymal stem cells for abdominal aortic aneurysm: A meta-analysis of preclinical studies. Stem Cell Res. Ther., Vol. 13. 10.1186/s13287-022-02755-w.
8. Wang, Y., H. Yi and Y. Song, 2021. The safety of MSC therapy over the past 15 years: A meta-analysis. Stem Cell Res. Ther., Vol. 12. 10.1186/s13287-021-02609-x.
9. Li, Y., F. Wang, H. Liang, D. Tang and M. Huang *et al*., 2021. Efficacy of mesenchymal stem cell transplantation therapy for type 1 and type 2 diabetes mellitus: A meta-analysis. Stem Cell Res. Ther., Vol. 12. 10.1186/s13287-021-02342-5.
10. Cui, J., L. Jin, M. Ding, J. He and L. Yang *et al*., 2022. Efficacy and safety of mesenchymal stem cells in the treatment of systemic sclerosis: A systematic review and meta-analysis. Stem Cell Res. Ther., Vol. 13. 10.1186/s13287-022-02786-3.
11. Chen, C.Y., W.C. Chen, C.K. Hsu, C.M. Chao and C.C. Lai, 2022. The clinical efficacy and safety of mesenchymal stromal cells for patients with COVID-19: A systematic review and meta-analysis of randomized controlled trials. J. Infect. Public Health, 15: 896-901.
12. Karaöz, E., P.C. Demircan, Ö. Sağlam, A. Aksoy, F. Kaymaz and G. Duruksu, 2011. Human dental pulp stem cells demonstrate better neural and epithelial stem cell properties than bone marrow-derived mesenchymal stem cells. Histochem. Cell. Biol., 136: 455-473.

13. Araldi, R.P., B.C. Prezoto, V. Gonzaga, B. Policiquio and T.B. Mendes *et al*., 2022. Advanced cell therapy with low tissue factor loaded product NestaCell® does not confer thrombogenic risk for critically ill COVID-19 heparin-treated patients. Biomed. Pharmacother., Vol. 149. 10.1016/j.biopha.2022.112920.
14. Kerkis, I., C.V. Wenceslau, D.M. Souza, N.C. Mambelli-Lisboa and L.H. Ynoue *et al*., 2022. Preclinical assessment of NestaCell® in Huntington's disease 3-NP rat model demonstrates restoration of BDNF, DARPP32, and D2R expression following intravenous single versus multiple injections. Cytotherapy, Vol. 24. 10.1016/S1465-3249(22)00855-6.
15. Kerkis, I. and A.I. Caplan, 2012. Stem cells in dental pulp of deciduous teeth. Tissue Eng. Part B: Rev., 18: 129-138.
16. Baydyuk, M. and B. Xu, 2014. BDNF signaling and survival of striatal neurons. Front. Cell. Neurosci., Vol. 8. 10.3389/fncel.2014.00254.
17. Bernal, A. and L. Arranz, 2018. Nestin-expressing progenitor cells: Function, identity and therapeutic implications. Cell. Mol. Life Sci., 75: 2177-2195.
18. Kerkis, I., A. Kerkis, D. Dozortsev, G.C. Stukart-Parsons and S.M.G. Massironi *et al*., 2007. Isolation and characterization of a population of immature dental pulp stem cells expressing OCT-4 and other embryonic stem cell markers. Cells Tissues Organs, 184: 105-116.
19. Lan, X., Z. Sun, C. Chu, J. Boltze and S. Li, 2019. Dental pulp stem cells: An attractive alternative for cell therapy in ischemic stroke. Front. Neurol., Vol. 10. 10.3389/fneur.2019.00824.
20. Wenceslau, C.V., D.M. de Souza, N.C. Mambelli-Lisboa, L.H. Ynoue and R.P. Araldi *et al*., 2022. Restoration of BDNF, DARPP32, and D2R expression following intravenous infusion of human immature dental pulp stem cells in Huntington's disease 3-NP rat model. Cells, Vol. 11. 10.3390/cells11101664.
21. Dominici, M., K. le Blanc, I. Mueller, I. Slaper-Cortenbach and F. Marini *et al*., 2006. Minimal criteria for defining multipotent mesenchymal stromal cells. The International Society for Cellular Therapy position statement. Cytotherapy, 8: 315-317.
22. Viswanathan, S., Y. Shi, J. Galipeau, M. Krampera and K. Leblanc *et al*., 2019. Mesenchymal stem versus stromal cells: International Society for Cell & Gene Therapy (ISCT®) Mesenchymal Stromal Cell committee position statement on nomenclature. Cytotherapy, 21: 1019-1024.
23. Fawzy El-Sayed, K.M., P. Klingebiel and C.E. Dörfer, 2016. Toll-like receptor expression profile of human dental pulp stem/progenitor cells. J. Endodontics, 42: 413-417.
24. Andrukhov, O., C. Behm, A. Blufstein and X. Rausch-Fan, 2019. Immunomodulatory properties of dental tissue-derived mesenchymal stem cells: Implication in disease and tissue regeneration. World J. Stem Cells, 11: 604-617.
25. Lizier, N.F., A. Kerkis, C.M. Gomes, J. Hebling, C.F. Oliveira, A.I. Caplan and I. Kerkis, 2012. Scaling-up of dental pulp stem cells isolated from multiple niches. PLoS ONE, Vol. 7. 10.1371/journal.pone.0039885.
26. Dadon-Nachum, M., K. Ben-Yaacov, T. Ben-Zur, Y. Barhum, D. Yaffe, E. Perlson and D. Offen, 2015. Transplanted modified muscle progenitor cells expressing a mixture of neurotrophic factors delay disease onset and enhance survival in the SOD1 mouse model of ALS. J. Mol. Neurosci., 55: 788-797.
27. Araldi, R.P., A.T. Ramos, A.L. Alievi, B. Policíquio, M.R. Teixei and T.B. Mendes *et al*., 2022. NestaCell® promotes motor, cognitive and neuropsychiatric functions amelioration and dopaminergic neurons restoration in a pre-clinical model of Parkinson's disease. Cytotherapy, Vol. 24. 10.1016/S1465-3249(22)00849-0.
28. Gonzaga, V.F., C.V. Wenceslau, D.P. Vieira, B. de Oliveira Policiquio, C. Khalil, R.P. Araldi and I. Kerkis, 2022. Therapeutic potential of human immature dental pulp stem cells observed in mouse model for acquired aplastic anemia. Cells, Vol. 11. 10.3390/cells11142252.
29. de Almeida, F.M., S.A. Marques, B. dos Santos Ramalho, R.F. Rodrigues and D.V. Cadilhe *et al*., 2011. Human dental pulp cells: A new source of cell therapy in a mouse model of compressive spinal cord injury. J. Neurotrauma, 28: 1939-1949.

30. Conesa, A., P. Madrigal, S. Tarazona, D. Gomez-Cabrero and A. Cervera *et al*., 2016. A survey of best practices for RNA-seq data analysis. Genome Biol., Vol. 17. 10.1186/s13059-016-0881-8.
31. Dobin, A., C.A. Davis, F. Schlesinger, J. Drenkow and C. Zaleski *et al*., 2013. STAR: Ultrafast universal RNA-seq aligner. Bioinformatics, 29: 15-21.
32. Love, M.I., W. Huber and S. Anders, 2014. Moderated estimation of fold change and dispersion for RNA-seq data with DESeq2. Genome Biol., Vol. 15. 10.1186/s13059-014-0550-8.
33. Tarazona, S., P. Furió-Tarí, D. Turrà, A.D. Pietro, M.J. Nueda, A. Ferrer and A. Conesa, 2015. Data quality aware analysis of differential expression in RNA-seq with NOISeq R/Bioc package. Nucleic Acids Res., Vol. 43. 10.1093/nar/gkv711.
34. McInnes, L., J. Healy and J. Melville, 2018. UMAP: Uniform manifold approximation and projection for dimension reduction. Arxiv, Vol. 3. 10.48550/arXiv.1802.03426.
35. Lamas, J.R., B. Fernandez-Gutierrez, A. Mucientes, F. Marco and Y. Lopiz *et al*., 2019. RNA sequencing of mesenchymal stem cells reveals a blocking of differentiation and immunomodulatory activities under inflammatory conditions in rheumatoid arthritis patients. Arthritis Res. Ther., Vol. 21. 10.1186/s13075-019-1894-y.
36. Walker, A.K., K.J. Spiller, G. Ge, A. Zheng and Y. Xu *et al*., 2015. Functional recovery in new mouse models of ALS/FTLD after clearance of pathological cytoplasmic TDP-43. Acta Neuropathol., 130: 643-660.
37. Narbute, K., V. Piļipenko, J. Pupure, Z. Dzirkale and U. Jonavičė *et al*., 2019. Intranasal administration of extracellular vesicles derived from human teeth stem cells improves motor symptoms and normalizes tyrosine hydroxylase expression in the substantia nigra and striatum of the 6-hydroxydopamine-treated rats. Stem Cells Transl. Med., 8: 490-499.
38. Monteiro, B.G., R.C. Serafim, G.B. Melo, M.C.P. Silva and N.F. Lizier *et al*., 2009. Human immature dental pulp stem cells share key characteristic features with limbal stem cells. Cell Proliferation, 42: 587-594.
39. Feitosa, M.L.T., C.A.P. Sarmento, R.Z. Bocabello, P.C.B. Beltrão-Braga and G.C. Pignatari *et al*., 2017. Transplantation of human immature dental pulp stem cell in dogs with chronic spinal cord injury. Acta Cir. Bras., 32: 540-549.
40. Gomes, J.Á.P., B.G. Monteiro, G.B. Melo, R.L. Smith and M.C.P. da Silva *et al*., 2010. Corneal reconstruction with tissue-engineered cell sheets composed of human immature dental pulp stem cells. Invest. Ophthalmol. Visual Sci., 51: 1408-1414.
41. Macedo, J., E. Pagani, C.V. Wenceslau, L. Ferrara and I. Kerkis, 2021. A phase I clinical trial on intravenous administration of immature human dental pulp stem cells (NestaCell HDTM) to Huntington's disease patients. Cytotherapy, Vol. 23. 10.1016/j.jcyt.2021.02.008.
42. Canals, J.M., J.R. Pineda, J.F. Torres-Peraza, M. Bosch and R. Martín-Ibañez *et al*., 2004. Brain-derived neurotrophic factor regulates the onset and severity of motor dysfunction associated with enkephalinergic neuronal degeneration in Huntington's disease. J. Neurosci., 24: 7727-7739.
43. Giampà, C., E. Montagna, C. Dato, M.A.B. Melone, G. Bernardi and F.R. Fusco, 2013. Systemic delivery of recombinant brain derived neurotrophic factor (BDNF) in the R6/2 mouse model of Huntington's disease. PLoS ONE, Vol. 11. 10.1371/journal.pone.0064037.
44. Zuccato, C. and E. Cattaneo, 2009. Brain-derived neurotrophic factor in neurodegenerative diseases. Nat. Rev. Neurol., 5: 311-322.
45. Chandwani, S., S. Keilani, M. Ortiz-Virumbrales, A. Morant, S. Bezdecny and M.E. Ehrlich, 2013. Induction of DARPP-32 by brain-derived neurotrophic factor in striatal neurons *in vitro* is modified by histone deacetylase inhibitors and Nab2. PLoS ONE, Vol. 8. 10.1371/journal.pone.0076842.
46. Hara, M., R. Fukui, E. Hieda, M. Kuroiwa and H.S. Bateup *et al*., 2010. Role of adrenoceptors in the regulation of dopamine/DARPP-32 signaling in neostriatal neurons. J. Neurochem., 113: 1046-1059.
47. Kerkis, I., J.M. da Silva, C.V. Wenceslau, N.C. Mambelli-Lisboa and E.O. Frare, 2020. Brain-Derived Neurotrophic Factor and Stem Cell-Based Technologies in Huntington's Disease Therapy. In: Neurodegenerative Diseases-Molecular Mechanisms and Current Therapeutic Approaches, Tunalı, N.E. (Ed.), IntechOpen, London, UK, ISBN: 978-1-83880-150-2.

48. Xie, Y., M.R. Hayden and B. Xu, 2010. BDNF overexpression in the forebrain rescues Huntington's disease phenotypes in YAC128 mice. J. Neurosci., 30: 14708-14718.
49. Gcwensa, N.Z., D.L. Russell, R.M. Cowell and L.A. Volpicelli-Daley, 2021. Molecular mechanisms underlying synaptic and axon degeneration in Parkinson's disease. Front. Cell. Neurosci., Vol. 15. 10.3389/fncel.2021.626128.
50. Bae, J.R. and S.H. Kim, 2017. Synapses in neurodegenerative diseases. BMB Rep., 50: 237-246.
51. Milnerwood, A.J. and L.A. Raymond, 2010. Early synaptic pathophysiology in neurodegeneration: Insights from Huntington's disease. Trends Neurosci., 33: 513-523.
52. Keshtkar, S., N. Azarpira and M.H. Ghahremani, 2018. Mesenchymal stem cell-derived extracellular vesicles: Novel frontiers in regenerative medicine. Stem Cell Res. Ther., Vol. 9. 10.1186/s13287-018-0791-7.
53. Qiu, G., G. Zheng, M. Ge, J. Wang, R. Huang, Q. Shu and J. Xu, 2018. Mesenchymal stem cell-derived extracellular vesicles affect disease outcomes via transfer of microRNAs. Stem Cell Res. Ther., Vol. 9. 10.1186/s13287-018-1069-9.
54. Zhu, S., X. Hu, S. Bennett, J. Xu and Y. Mai, 2022. The molecular structure and role of humanin in neural and skeletal diseases, and in tissue regeneration. Front. Cell Dev. Biol., Vol. 10. 10.3389/fcell.2022.823354.
55. Hashimoto, Y., M. Kurita, S. Aiso, I. Nishimoto and M. Matsuoka, 2009. Humanin inhibits neuronal cell death by interacting with a cytokine receptor complex or complexes involving CNTF Receptor α/WSX-1/gp130. Mol. Biol. Cell, 20: 2864-2873.
56. Harada, M., Y. Habata, M. Hosoya, K. Nishi, R. Fujii, M. Kobayashi and S. Hinuma, 2004. N-Formylated humanin activates both formyl peptide receptor-like 1 and 2. Biochem. Biophys. Res. Commun., 324: 255-261.
57. Zhai, D., F. Luciano, X. Zhu, B. Guo, A.C. Satterthwait and J.C. Reed, 2005. Humanin binds and nullifies bid activity by blocking its activation of Bax and Bak. J. Biol. Chem., 280: 15815-15824.
58. Morris, D.L., D.W. Kastner, S. Johnson, M.P. Strub and Y. He *et al*., 2019. Humanin induces conformational changes in the apoptosis regulator BAX and sequesters it into fibers, preventing mitochondrial outer-membrane permeabilization. J. Biol. Chem., 294: 19055-19065.
59. Morris, D.L., S. Johnson, C.K.E. Bleck, D.Y. Lee and N. Tjandra, 2020. Humanin selectively prevents the activation of pro-apoptotic protein BID by sequestering it into fibers. J. Biol. Chem., 295: 18226-18238.
60. Hashimoto, Y., Y. Takeshita, M. Naito, H. Uchino and M. Matsuoka, 2014. Apollon/Bruce is upregulated by Humanin. Mol. Cell. Biochem., 397: 147-155.
61. Sreekumar, P.G., K. Ishikawa, C. Spee, H.H. Mehta and J. Wan *et al*., 2016. The mitochondrial-derived peptide humanin protects RPE cells from oxidative stress, senescence, and mitochondrial dysfunction. Invest. Ophthalmol. Visual Sci., 57: 1238-1253.
62. Teleanu, D.M., A.G. Niculescu, I.I. Lungu and C.I. Radu *et al*., 2022. An overview of oxidative stress, neuroinflammation, and neurodegenerative diseases. Int. J. Mol. Sci., Vol. 23. 10.3390/ijms23115938.